Journal of Computational and Applied Mathematics 356 (2019) 198–218

Contents lists available at ScienceDirect

Journal of Computational and Applied Mathematics

journal homepage: www.elsevier.com/locate/cam

Error estimates and post-processing of local discontinuous Galerkin method for Schrödinger equations

Qi Tao, Yinhua Xia *,[1]

School of Mathematical Sciences, University of Science and Technology of China, Hefei, Anhui 230026, PR China

ARTICLE INFO

Article history:
Received 6 March 2018
Received in revised form 19 October 2018

Keywords:
Local discontinuous Galerkin method
Error estimates
Negative-order norm
Schrödinger equations
SIAC filter
Post-processing

ABSTRACT

In this paper, we present L^2 and negative-order norm estimates for the local discontinuous Galerkin (LDG) method solving variable coefficient Schrödinger equations. For these special solutions the LDG method exhibits "hidden accuracy", and we are able to extract it through the use of a convolution kernel that is composed of a linear combination of B-splines. This technical was initially introduced by Cockburn, Luskin, Shu, and Süli for linear hyperbolic equations and extended by Ryan et al. as a smoothness-increasing accuracy-conserving (SIAC) filter. We demonstrate that it is possible to extend the SIAC filter on Schrödinger equations. When polynomials of degree k are used, we can prove theoretically the LDG method solutions are of order $k+1$, whereas the post-processed solutions that convolution with the SIAC filter are of order at least $2k$. Additionally, we present numerical results to confirm that the accuracy of LDG solutions can be improved from $\mathbb{O}(h^{k+1})$ to at least $\mathbb{O}(h^{2k+1})$ for Schrödinger equations by using alternating numerical fluxes.

1. Introduction

In this paper, we consider the accuracy enhancement of the local discontinuous Galerkin (LDG) method solving variable coefficient Schrödinger equations with smooth solutions

$$iu_t + \Delta u - V(\boldsymbol{x})u = 0, \quad (\boldsymbol{x}, t) \in \Omega \times (0, T], \tag{1.1}$$

$$u(\boldsymbol{x}, 0) = u_0(\boldsymbol{x}). \tag{1.2}$$

Here $i = \sqrt{-1}$ is the complex unity, t is the time variable, $\boldsymbol{x} = (x_1, \ldots, x_d)$, $d \leq 3$ represents the spatial dimension, $u(\boldsymbol{x}, t)$ is a complex wave function, and $V(\boldsymbol{x})$ is a given real value electrostatic potential. The accuracy enhancement technique is based on the a priori L^2 and negative-order norm error estimates for the LDG method. In these estimates, we concentrate on the method in the interior of the domain and neglect the effect of the boundary terms, therefore we always consider the periodic boundary conditions, also, assuming the initial condition $u_0(\boldsymbol{x})$ is a smooth function.

The time dependent Schrödinger equations can describe many phenomena, and have many significant applications in optics, seismology and plasma physics, especially in describing the quantum state of a physical system over the time, but we can hardly get the solution exactly. To solve this problem many numerical methods have been investigated, we implement the local discontinuous Galerkin (LDG) method [1,2] in this paper. Discontinuous Galerkin methods (DG) are a class of finite

* Corresponding author.
E-mail addresses: taoq@mail.ustc.edu.cn (Q. Tao), yhxia@ustc.edu.cn (Y. Xia).

[1] Research supported by NSFC Grant Nos. 11471306, 11871449, and a grant from the Science & Technology on Reliability & Environmental Engineering Laboratory (No. 6142A0502020817).

https://doi.org/10.1016/j.cam.2019.01.033
0377-0427/

element methods using completely discontinuous basis functions. The first DG method was introduced in 1973 by Reed and Hill [3], in the framework of neutron transport, i.e. a time independent linear hyperbolic equation. It was first developed for hyperbolic conservation laws by Cockburn et al. The LDG method is an extension of the DG method, aimed at solving partial differential equations (PDEs) containing higher than first order spatial derivatives. The LDG method was constructed by Cockburn and Shu [4] to solve nonlinear convection diffusion equations containing second order spatial derivatives. The idea of the LDG method is to rewrite the equations with higher order derivatives into a first order system, then apply the DG method on the system. The design of the numerical fluxes is the key ingredient to ensure stability. The LDG method is particularly a nice method that is suitable for unstructured meshes as well as parallelization due to the properties of the approximation space and the choice of numerical flux, and it has been developed for various high order PDEs. We refer reader to [5–7] and the review paper [8] for more details about the recent development of DG and LDG methods.

In [1] Xu and Shu developed the LDG method to solve the nonlinear Schrödinger equations, and they proved $k+1$ order of accuracy where k is the highest order of the approximation polynomials for the linear Schrödinger equation [2], when alternating flux was used. In this paper we consider the a priori error estimate for the variable coefficient Schrödinger equations and the negative-order norm estimate. Since the DG methods use piecewise polynomial to approximate the solution of a differential equation over a domain, the inter-element discontinuities are usually problematic in error estimates. The local post-processing technique can make use of the information contained in the negative-order norm, to improve the continuity and degree of the DG approximations while preserving and extracting the superconvergence of the original DG approximations. This technique was firstly developed by Bramble and Schatz for the continuous finite element methods [9] in 1977, further studied by Thomée to obtain a similar superconvergence order approximation for derivatives in [10]. In 1978 Mock and Lax deduced this technique from another point of view by studying the discontinuous solution of linear hyperbolic equation [11]. Cockburn, Luskin, Shu and Süli [12] initially introduced this technique for linear hyperbolic equations with periodic boundary conditions, in the context of the discontinuous Galerkin methods. The superconvergence rate of $2k+1$ is proven in the negative order norm. Later Shu and Ryan [13] proposed the idea of one-side post-processing technique, which can be applied to the boundary regions, discontinuities, and interface of the elements.

Furthermore, this technique is labeled as a smoothness-increasing accuracy-conserving (SIAC) filter by Kirby, Ryan et al. [14]. This one-side idea was modified in [15] and named as a position-dependent filter to deal with the non-periodic boundary. It was also extended to the nonuniform mesh [16], and different kinds of element including quadrilateral, structure triangular, tetrahedral and even unstructured triangular mesh [17–19]. This technique can also be used to deal with the nonlinear equations, in [20] Ji et al. proved the negative-norm estimate for nonlinear hyperbolic conservational laws, later Meng and Ryan analyzed the divided difference estimate for nonlinear hyperbolic conservation laws [21]. There are a wide variety of studies using this post-processing technique, such as applied to an aeroacoustic problem [22], derivatives in the DG approximation [23,24], convection–diffusion equations [25], and streamline visualization [14,26].

We would like to mention briefly recent superconvergence results for finite element methods to Schrödinger equations. In [27] Zhou et al. build a special interpolation function by construction a correction function, thus establish a strong $2k+1$ order superconvergence between the numerical solution of the LDG method and the interpolation function, and in some special points the function value and the derivative approximation also have some superconvergence. In [28] Huang et al. considered the continuous finite element method for two-dimensional Schrödinger equations, and discussed the superconvergence error estimate in H^1 norm. In [29] Shi et al. used a nonconforming quadrilateral Wilson type finite element approximation to Schrödinger equations and proved its second order superconvergence in H^1 norm. In this paper, we estimate the L^2 error, and use a technical of dual argument to present an analysis of the negative-order norm for solutions obtained via the local discontinuous Galerkin method for solving variable coefficient Schrödinger equations. We obtain at least $2k$ order of accuracy in the negative-order norm, and $k+1$ order in the L^2-norm, when the alternating flux was used. By using SIAC filter we can confirm numerically that at least $2k+1$ order can be obtained after the post-processing.

The paper is organized as follows. In Section 2, we define relevant notations, definitions and projections that will be used in the proof of the LDG method. In Section 3, we introduce the LDG method and the L^2 error estimate for variable coefficient Schrödinger equations. In Section 4, we prove the superconvergence of the LDG solutions for Schrödinger equations in negative-order norm. And these results are confirmed numerically in Section 5. In Section 6, we give some concluding remarks.

2. Notations, definitions and projections

We begin by defining some necessary notations, definitions and projections used in the proof of L^2 and negative-order norms error estimates for the local discontinuous Galerkin method solving Schrödinger equations.

2.1. Tessellation and function spaces

Let $\mathcal{I}_h$ denote a tessellation of Ω with shape-regular elements K, invariant under translations, and the union of the boundary face of element $K \in \mathcal{I}_h$, denoted as $\Gamma = \cup_{K\in\mathcal{I}_h} \partial K$. We only consider the uniform Cartesian mesh of size h in this paper.

Since the approximation space in discontinuous Galerkins methods consists of piecewise polynomials, we need to have a way of denoting the value of the approximation on the "left" and "right" side of an element boundary, e. We give the

designation K_L for element to the left side of the e, and K_R for element to the right side of the e, following the notation in [1] and [30]. The normal vectors ν_L and ν_R on the edge e point exterior to K_L and K_R respectively. Assuming ψ is a function defined on K_L and K_R, let ψ^- denote $(\psi|_{K_L})|_e$ and ψ^+ denote $(\psi|_{K_R})|_e$, the right and left traces, respectively.

Let $\mathcal{Q}^k(K)$ be the space of tensor product of polynomials of degree at most $k \geq 0$ on $K \in \mathcal{I}_h$ in each variable. The finite element spaces are denoted by

$$V_h = \{\eta \in L^2(\Omega) : \eta|_K \in \mathcal{Q}^k(K), \forall K \in \mathcal{I}_h\},$$
$$\Sigma_h = \{\boldsymbol{\Phi} = (\Phi_1, \ldots, \Phi_d) \in (L^2(\Omega))^d : \Phi_l|_K \in \mathcal{Q}^k(K), l = 1 \ldots d, \forall K \in \mathcal{I}_h\}.$$

For the one-dimensional case, $\mathcal{Q}^k(K) = \mathcal{P}^k$ which is the polynomial space of degree at most k.

2.2. Inner products and norms

We next define the L^2 and the Sobolev norms used in this paper. Additionally we define the negative-order Sobolev norm. We define the inner product as

$$(\omega, v)_\Omega = \sum_K \int_K \omega v dK, \qquad (\omega, v)_\Gamma = \sum_K \int_{\partial K} \omega v ds, \tag{2.3}$$

$$(\mathbf{p}, \mathbf{q})_\Omega = \sum_K \int_K \mathbf{p} \cdot \mathbf{q} dK, \qquad (\mathbf{p}, \mathbf{q})_\Gamma = \sum_K \int_{\partial K} \mathbf{p} \cdot \mathbf{q} ds, \tag{2.4}$$

for the scalar real functions ω, v and vector real functions $\mathbf{p}$, $\mathbf{q}$ respectively. The definitions used for the L^2-norm in Ω and on the boundary are given by

$$\|\omega\|_\Omega^2 = \int_\Omega |\omega|^2 d\mathbf{x}, \qquad \|\mathbf{q}\|_\Omega^2 = \int_\Omega |\mathbf{q}|^2 d\mathbf{x}, \tag{2.5}$$

and

$$\|\eta\|_\Gamma^2 = \sum_K \int_{\partial K} |\eta|^2 ds, \qquad \|\mathbf{q}\|_\Gamma^2 = \sum_K \int_{\partial K} |\mathbf{q}|^2 ds. \tag{2.6}$$

The $H^l(K)$-norm over K is

$$\|\eta\|_{l,K} = (\sum_{|\alpha| \leq l} \|D^\alpha \eta\|_K^2)^{\frac{1}{2}}, \quad l \geq 0. \tag{2.7}$$

We denote the norm in domain Ω in the following way

$$\|\eta\|_{l,\Omega} = (\sum_{K \in \mathcal{I}_h} \|\eta\|_{l,K}^2)^{\frac{1}{2}}, \qquad \|\mathbf{q}\|_{l,\Omega} = (\sum_{K \in \mathcal{I}_h} \|\mathbf{q}\|_{l,K}^2)^{\frac{1}{2}}, \quad l \geq 0. \tag{2.8}$$

The negative-order norm is defined as:

$$\|\eta\|_{-l,\Omega} = \sup_{\Phi \in \mathcal{C}_0^\infty} \frac{(\eta, \Phi)_\Omega}{\|\Phi\|_{l,\Omega}}, \quad l \geq 0. \tag{2.9}$$

We note that the definition is simplified for those norms and only designate the norm type and not on domain.

2.3. Projections and interpolation properties

In what follows, we will consider the standard L^2-projections P_k for the scalar functions and Π_k for vector-valued functions, and we have the following error estimates ([31] Chapter 3)

$$\|\xi^e\|_\Omega + h^{\frac{d}{2}} \|\xi^e\|_{L^\infty(\Omega)} + h^{\frac{1}{2}} \|\xi^e\|_\Gamma \leq C h^{k+1} \|\xi\|_{H^{k+1}(\Omega)}, \quad \forall \xi \in H^{k+1}(\Omega), \tag{2.10}$$

$$\|\boldsymbol{\rho}^e\|_\Omega + h^{\frac{d}{2}} \|\boldsymbol{\rho}^e\|_{L^\infty(\Omega)} + h^{\frac{1}{2}} \|\boldsymbol{\rho}^e\|_\Gamma \leq C h^{k+1} \|\boldsymbol{\rho}\|_{H^{k+1}(\Omega)}, \quad \forall \boldsymbol{\rho} \in [H^{k+1}(\Omega)]^d, \tag{2.11}$$

where $\xi^e = P_k \xi - \xi$, $\boldsymbol{\rho}^e = \Pi_k \boldsymbol{\rho} - \boldsymbol{\rho}$. We note that the positive constant C is independent of h.

And two special projections $P^\pm$ and $\Pi^\pm$, in the one-dimensional case,

$$P^\pm : H^1(\Omega) \to V_h,$$

which are defined as follows. Given a function $\xi \in H^1(\Omega)$, and an arbitrary subinterval $K_j = (x_{j-\frac{1}{2}}, x_{j+\frac{1}{2}})$, the restriction of $P^\pm \xi$ to subinterval K_j are defined as the elements of $\mathcal{P}^k(K_j)$ that satisfy

$$\int_{K_j} (P^+ \xi - \xi) \omega dx = 0, \quad \forall \omega \in \mathcal{P}^{k-1}(K_j), \qquad \text{and} \qquad P^+ \xi(x_{j-\frac{1}{2}}) = \xi(x_{j-\frac{1}{2}}),$$

$$\int_{K_j}(P^-\xi-\xi)\omega dx=0,\quad \forall\omega\in\mathcal{P}^{k-1}(K_j),\qquad \text{and}\qquad P^-\xi(x_{j+\frac{1}{2}})=\xi(x_{j+\frac{1}{2}}),$$

and $\Pi^\pm=P^\pm$ in one dimension. Similar to the one-dimensional case, we can define the projections for two-dimensional problems in Cartesian meshes. The projections $P^\pm$ for scalar functions are defined as

$$P^\pm=P_x^\pm\otimes P_y^\pm, \tag{2.12}$$

where the subscripts x and y indicate the one-dimensional projections [2,32]. The projections $\Pi^\pm$ for the vector-valued function $\boldsymbol{\rho}=(\rho_1(x,y),\rho_2(x,y))\in H^1(K)^2$ are defined as

$$\Pi^\pm\boldsymbol{\rho}=(P_x^\pm\otimes(P_k)_y\rho_1,(P_k)_x\otimes P_y^\pm\rho_2). \tag{2.13}$$

Here $(P_k)_x$ and $(P_k)_y$ are the standard L^2-projections in the x and y directions, respectively [2,33].

For the definition of similar projections for the three-dimensional case we refer to [33], and for the projections mentioned above, there exists a constant C independent of h such that [31]

$$\|\xi^e\|_\Omega\le Ch^{k+1}\|\xi\|_{H^{k+1}(\Omega)},\quad \forall\xi\in H^{k+1}(\Omega),$$
$$\|\boldsymbol{\rho}^e\|_\Omega\le Ch^{k+1}\|\boldsymbol{\rho}\|_{H^{k+1}(\Omega)},\quad \forall\boldsymbol{\rho}\in[H^{k+1}(\Omega)]^d,$$

where $\xi^e=P^\pm\xi-\xi$, $\boldsymbol{\rho}^e=\Pi^\pm\boldsymbol{\rho}-\boldsymbol{\rho}$.

The projection P^- on the Cartesian meshes has the following superconvergence property.

Lemma 2.1. *Suppose $\xi\in H^{k+2}(\Omega)$, $\boldsymbol{\rho}\in\Sigma_h$, and the projection P^-, then we have*

$$|(\xi-P^-\xi,\nabla\cdot\boldsymbol{\rho})_\Omega-(\xi-\widehat{P^-\xi},\boldsymbol{\rho}\cdot\nu)_\Gamma|\le Ch^{k+1}\|\xi\|_{H^{k+2}(\Omega)}\|\boldsymbol{\rho}\|_\Omega, \tag{2.14}$$

where the "hat" term is the numerical flux ($\widehat{\psi}=\psi^-$), and C is independent of h. Similar results hold for the projections P^+ and $\Pi^\pm$ with proper numerical fluxes.

2.4. Regularity for the Schrödinger equations

We need to establish a regularity result that is used to complete the negative-order norm error estimates of the variable coefficient Schrödinger equations, that is:

Lemma 2.2. *Consider the variable coefficient Schrödinger equations (1.1) with smooth initial condition (1.2), and periodic boundary conditions, and $V(\mathbf{x})$ is a given smooth real function, then the solution to (1.1) satisfies the following regularity property*

$$\|u(x,t)\|_{l,\Omega}\le C\|u(x,0)\|_{l,\Omega}, \tag{2.15}$$

for $l\ge 0$, where the C is a constant that depends on $V(\mathbf{x})$.

We omit to provide a proof of this lemma as it can easily be obtained by using the energy estimate.

3. LDG scheme and L^2 error estimate

3.1. The LDG scheme for Schrödinger equation

In this section we define the local discontinuous Galerkin method for Schrödinger equation (1.1), with the smooth initial condition (1.2). Firstly we decompose the complex function $u(\boldsymbol{x},t)$ into its real and imaginary parts by

$$u(\boldsymbol{x},t)=r(\boldsymbol{x},t)+is(\boldsymbol{x},t),$$

where r and s are real functions. Under the new notation, problem (1.1) can be written as

$$r_t+\Delta s-V(\boldsymbol{x})s=0,\quad (x,t)\in\Omega\times(0,T], \tag{3.16}$$
$$s_t-\Delta r+V(\boldsymbol{x})r=0,\quad (x,t)\in\Omega\times(0,T], \tag{3.17}$$

with the smooth initial conditions

$$r(\boldsymbol{x},0)=r_0(\boldsymbol{x}),\qquad s(\boldsymbol{x},0)=s_0(\boldsymbol{x}), \tag{3.18}$$

and the periodic boundary conditions. Then we write (3.16) and (3.17) as an equivalent first-order system:

$$r_t+\nabla\cdot\mathbf{p}-V(\boldsymbol{x})s=0, \tag{3.19}$$
$$\mathbf{p}-\nabla s=0, \tag{3.20}$$

$$s_t - \nabla \cdot \mathbf{q} + V(\boldsymbol{x})r = 0, \tag{3.21}$$

$$\mathbf{q} - \nabla r = 0. \tag{3.22}$$

The LDG scheme is: Find $r_h, s_h \in V_h$ and $\mathbf{p}_h, \mathbf{q}_h \in \Sigma_h$ such that, for all test functions $\omega, v \in V_h$ and $\boldsymbol{\eta}, \boldsymbol{\xi} \in \Sigma_h$

$$((r_h)_t, \omega)_K - (\mathbf{p}_h, \nabla\omega)_K - (V(\boldsymbol{x})s_h, \omega)_K + (\widehat{\mathbf{p}_h} \cdot \boldsymbol{\nu}, \omega)_{\partial K} = 0, \tag{3.23}$$

$$(\mathbf{p}_h, \boldsymbol{\eta})_K + (s_h, \nabla \cdot \boldsymbol{\eta})_K - (\widehat{s_h}, \boldsymbol{\eta} \cdot \boldsymbol{\nu})_{\partial K} = 0, \tag{3.24}$$

$$((s_h)_t, v)_K + (\mathbf{q}_h, \nabla v)_K + (V(\boldsymbol{x})r_h, v)_K - (\widehat{\mathbf{q}_h} \cdot \boldsymbol{\nu}, v)_{\partial K} = 0, \tag{3.25}$$

$$(\mathbf{q}_h, \boldsymbol{\xi})_K + (r_h, \nabla \cdot \boldsymbol{\xi})_K - (\widehat{r_h}, \boldsymbol{\xi} \cdot \boldsymbol{\nu})_{\partial K} = 0. \tag{3.26}$$

Where $\boldsymbol{\nu}$ is the unit normal outward vector for the integration domain. The "hat" terms in the cell boundary from integration by parts are the "numerical fluxes", which are single-value functions defined on the edges and should be designed based on different guiding principles for different PDEs to ensure stability and local solvability of the intermediate variables $\mathbf{p}_h, \mathbf{q}_h$. It turns out that we can choose the alternating fluxes, i.e.,

$$\widehat{\mathbf{p}_h} = \mathbf{p}_h^+, \qquad \widehat{r_h} = r_h^-, \qquad \widehat{\mathbf{q}_h} = \mathbf{q}_h^+, \qquad \widehat{s_h} = s_h^-, \tag{3.27}$$

or

$$\widehat{\mathbf{p}_h} = \mathbf{p}_h^-, \qquad \widehat{r_h} = r_h^+, \qquad \widehat{\mathbf{q}_h} = \mathbf{q}_h^-, \qquad \widehat{s_h} = s_h^+. \tag{3.28}$$

Without loss of generality, in the next proof we take the first flux (3.27). Summing the scheme (3.23)–(3.26) over K, we obtain

$$((r_h)_t, \omega)_\Omega - B_1(\mathbf{p}_h, s_h, \omega) = 0, \tag{3.29}$$

$$(\mathbf{p}_h, \boldsymbol{\eta})_\Omega + B_2(s_h, \boldsymbol{\eta}) = 0, \tag{3.30}$$

$$((s_h)_t, v)_\Omega + B_1(\mathbf{q}_h, r_h, v) = 0, \tag{3.31}$$

$$(\mathbf{q}_h, \boldsymbol{\xi})_\Omega + B_2(r_h, \boldsymbol{\xi}) = 0, \tag{3.32}$$

where B_1, and B_2 are defined as

$$B_1(\mathbf{p}_h, s_h, \omega) = (\mathbf{p}_h, \nabla\omega)_\Omega + (V(\mathbf{x})s_h, \omega)_\Omega - \sum_K (\widehat{\mathbf{p}_h} \cdot \nu, \omega)_{\partial K},$$

$$B_2(s_h, \boldsymbol{\eta}) = (s_h, \nabla \cdot \boldsymbol{\eta})_\Omega - \sum_K (\widehat{s_h}, \boldsymbol{\eta} \cdot \nu)_{\partial K}.$$

3.2. L^2 error estimate

In what follows, we will give the L^2 error estimate for the LDG scheme (3.23)–(3.26). In the paper of Xu and Shu ([2], Theorem 4.4), they have given the optimal L^2 convergence result for the linear Schrödinger equation ($V(\mathbf{x}) = 0$). We obtain the same optimal result for the variable coefficient Schrödinger equations.

Theorem 3.1. *For $0 < T < T^*$ where T^* is the maximal time of the classical solution, let r and s be the exact solutions of the problem (3.16) and (3.17), with the smooth initial conditions (3.18) and periodic boundary conditions. Furthermore, let $V(x)$ be a smooth real function, and $r_h, s_h, \mathbf{p}_h, \mathbf{q}_h$ are solutions to (3.23)–(3.26) then*

$$\|r - r_h\|_{L^\infty((0,T);L^2(\Omega))} \le Ch^{k+1}, \qquad \|s - s_h\|_{L^\infty((0,T);L^2(\Omega))} \le Ch^{k+1}, \tag{3.33}$$

$$\|\mathbf{p} - \mathbf{p}_h\|_{L^\infty((0,T);L^2(\Omega))} \le Ch^{k+1}, \qquad \|\mathbf{q} - \mathbf{q}_h\|_{L^\infty((0,T);L^2(\Omega))} \le Ch^{k+1}, \tag{3.34}$$

where the constant C depends on T, r and s and is independent of h.

Firstly we need the error equations. Notice that the scheme (3.23)–(3.26) are also satisfied when the numerical solutions $r_h, s_h, \mathbf{p}_h, \mathbf{q}_h$ are replaced by the exact solution $r, s, \mathbf{p} = \nabla s, \mathbf{q} = \nabla r$, then we have the error equations

$$((r - r_h)_t, \omega)_K - (\mathbf{p} - \mathbf{p}_h, \nabla\omega)_K - (V(\boldsymbol{x})(s - s_h), \omega)_K + ((\mathbf{p} - \widehat{\mathbf{p}_h}) \cdot \boldsymbol{\nu}, \omega)_{\partial K} = 0, \tag{3.35}$$

$$(\mathbf{p} - \mathbf{p}_h, \boldsymbol{\eta})_K + (s - s_h, \nabla \cdot \boldsymbol{\eta})_K - (s - \widehat{s_h}, \boldsymbol{\eta} \cdot \boldsymbol{\nu})_{\partial K} = 0, \tag{3.36}$$

$$((s - s_h)_t, v)_K + (\mathbf{q} - \mathbf{q}_h, \nabla v)_K + (V(\boldsymbol{x})(r - r_h), v)_K - ((\mathbf{q} - \widehat{\mathbf{q}_h}) \cdot \boldsymbol{\nu}, v)_{\partial K} = 0, \tag{3.37}$$

$$(\mathbf{q} - \mathbf{q}_h, \boldsymbol{\xi})_K + (r - r_h, \nabla \cdot \boldsymbol{\xi})_K - (r - \widehat{r_h}, \boldsymbol{\xi} \cdot \boldsymbol{\nu})_{\partial K} = 0. \tag{3.38}$$

Denote

$$\mathbf{e}_r = r - r_h = r - Pr + Pr - r_h = r - Pr + P\mathbf{e}_r, \tag{3.39}$$

$$\mathbf{e}_{\mathbf{p}} = \mathbf{p} - \mathbf{p}_h = \mathbf{p} - \Pi\mathbf{p} + \Pi\mathbf{p} - \mathbf{p}_h = \mathbf{p} - \Pi\mathbf{p} + \Pi\mathbf{e}_{\mathbf{p}}, \tag{3.40}$$

$$\mathbf{e}_s = s - s_h = s - Ps + Ps - s_h = s - Ps + P\mathbf{e}_s, \tag{3.41}$$

$$\mathbf{e}_{\mathbf{q}} = \mathbf{q} - \mathbf{q}_h = \mathbf{q} - \Pi\mathbf{q} + \Pi\mathbf{q} - \mathbf{q}_h = \mathbf{q} - \Pi\mathbf{q} + \Pi\mathbf{e}_{\mathbf{q}}, \tag{3.42}$$

where P and Π are the projections onto the finite element space V_h and Σ_h, respectively. In this section we choose the projections as follows

$$(P, \Pi) = (P^-, P^+) \quad d = 1, \tag{3.43}$$

$$(P, \Pi) = (P^-, \Pi^+) \quad d = 2, 3. \tag{3.44}$$

We choose the initial conditions $r_h(x, 0) = P^+r(x, 0)$, $s_h(x, 0) = P^+s(x, 0)$, then we have the optimal error estimates for numerical initial conditions

$$\|r(x, 0) - r_h(x, 0)\| \le Ch^{k+1}, \qquad \|s(x, 0) - s_h(x, 0)\| \le Ch^{k+1}, \tag{3.45}$$

and

$$\|\mathbf{p}(x, 0) - \mathbf{p}_h(x, 0)\| \le Ch^{k+1}, \qquad \|\mathbf{q}(x, 0) - \mathbf{q}_h(x, 0)\| \le Ch^{k+1}. \tag{3.46}$$

3.2.1. The first energy equation

We first take the test functions $\omega = P\mathbf{e}_r$, $\boldsymbol{\eta} = \Pi\mathbf{e}_{\mathbf{q}}$, $v = P\mathbf{e}_s$, $\boldsymbol{\xi} = \Pi\mathbf{e}_{\mathbf{p}}$ in the LDG scheme, which results in

$$((r - r_h)_t, P\mathbf{e}_r)_\Omega - B_1(\mathbf{p} - \mathbf{p}_h, s - s_h, P\mathbf{e}_r) = 0, \tag{3.47}$$

$$(\mathbf{p} - \mathbf{p}_h, \Pi\mathbf{e}_{\mathbf{q}})_\Omega + B_2(s - s_h, \Pi\mathbf{e}_{\mathbf{q}}) = 0, \tag{3.48}$$

$$((s - s_h)_t, P\mathbf{e}_s)_\Omega + B_1(\mathbf{q} - \mathbf{q}_h, r - r_h, P\mathbf{e}_s) = 0, \tag{3.49}$$

$$(\mathbf{q} - \mathbf{q}_h, \Pi\mathbf{e}_{\mathbf{p}})_\Omega + B_2(r - r_h, \Pi\mathbf{e}_{\mathbf{p}}) = 0. \tag{3.50}$$

Then we sum (3.47)–(3.49) and minus (3.50), and it follows that

$$\begin{aligned}\frac{1}{2}\frac{d}{dt}\|P\mathbf{e}_r\|_\Omega^2 + \frac{1}{2}\frac{d}{dt}\|P\mathbf{e}_s\|_\Omega^2 = &-((r - Pr)_t, P\mathbf{e}_r)_\Omega + B_1(\mathbf{p} - \mathbf{p}_h, s - s_h, P\mathbf{e}_r) \\ &- ((s - Ps)_t, P\mathbf{e}_s)_\Omega - B_1(\mathbf{q} - \mathbf{q}_h, r - r_h, P\mathbf{e}_s) \qquad (3.51)\\ &- (\mathbf{p} - \Pi\mathbf{p}, \Pi\mathbf{e}_{\mathbf{q}})_\Omega - B_2(s - s_h, \Pi\mathbf{e}_{\mathbf{q}}) \qquad (3.52)\\ &+ (\mathbf{q} - \Pi\mathbf{q}, \Pi\mathbf{e}_{\mathbf{p}})_\Omega + B_2(r - r_h, \Pi\mathbf{e}_{\mathbf{p}}). \qquad (3.53)\end{aligned}$$

By the definitions of B_1 and B_2, we have

$$\begin{aligned}&B_1(\mathbf{p} - \mathbf{p}_h, s - s_h, P\mathbf{e}_r) + B_2(r - r_h, \Pi\mathbf{e}_{\mathbf{p}})\\
&= (\mathbf{p} - \Pi\mathbf{p} + \Pi\mathbf{e}_{\mathbf{p}}, \nabla P\mathbf{e}_r)_\Omega - \sum_K((\mathbf{p} - \widehat{\Pi\mathbf{p}} + \widehat{\Pi\mathbf{e}_{\mathbf{p}}}) \cdot \nu, P\mathbf{e}_r)_{\partial K} + (V(\mathbf{x})(s - s_h), P\mathbf{e}_r)_\Omega\\
&\quad + (r - Pr + P\mathbf{e}_r, \nabla \cdot \Pi\mathbf{e}_{\mathbf{p}})_\Omega - \sum_K(r - \widehat{Pr} + \widehat{P\mathbf{e}_r}, \Pi\mathbf{e}_{\mathbf{p}} \cdot \nu)_{\partial K}\\
&= (\Pi\mathbf{e}_{\mathbf{p}}, \nabla P\mathbf{e}_r)_\Omega - \sum_K(\widehat{\Pi\mathbf{e}_{\mathbf{p}}} \cdot \nu, P\mathbf{e}_r)_{\partial K} + (P\mathbf{e}_r, \nabla \cdot \Pi\mathbf{e}_{\mathbf{p}})_\Omega - \sum_K(\widehat{P\mathbf{e}_r}, \Pi\mathbf{e}_{\mathbf{p}} \cdot \nu)_{\partial K}\\
&\quad + \sum_K((\mathbf{p} - \Pi\mathbf{p}, \nabla P\mathbf{e}_r)_K - ((\mathbf{p} - \widehat{\Pi\mathbf{p}}) \cdot \nu, P\mathbf{e}_r)_{\partial K}) + (V(\mathbf{x})(s - s_h), P\mathbf{e}_r)_\Omega\\
&\quad + \sum_K((r - Pr, \nabla \cdot \Pi\mathbf{e}_{\mathbf{p}})_K - (r - \widehat{Pr}, \Pi\mathbf{e}_{\mathbf{p}} \cdot \nu)_{\partial K})\\
&= \sum_K((\mathbf{p} - \Pi\mathbf{p}, \nabla P\mathbf{e}_r)_K - ((\mathbf{p} - \widehat{\Pi\mathbf{p}}) \cdot \nu, P\mathbf{e}_r)_{\partial K}) + (V(\mathbf{x})(s - s_h), P\mathbf{e}_r)_\Omega\\
&\quad + \sum_K((r - Pr, \nabla \cdot \boldsymbol{\Pi}\mathbf{e}_{\mathbf{p}})_K - (r - \widehat{Pr}, \Pi\mathbf{e}_{\mathbf{p}} \cdot \nu)_{\partial K}). \qquad (3.54)\end{aligned}$$

The last equality is obtained by integrating by parts and periodic boundary conditions. Now we combine (3.51), (3.54) and it follows that

$$\begin{aligned}&\frac{1}{2}\frac{d}{dt}\|P\mathbf{e}_r\|_\Omega^2 + \frac{1}{2}\frac{d}{dt}\|P\mathbf{e}_s\|_\Omega^2\\
&= -((r - Pr)_t, P\mathbf{e}_r)_\Omega + \sum_K((\mathbf{p} - \Pi\mathbf{p}, \nabla P\mathbf{e}_r)_K - ((\mathbf{p} - \widehat{\Pi\mathbf{p}}) \cdot \nu, P\mathbf{e}_r)_{\partial K})\end{aligned}$$

$$
\begin{aligned}
&+\sum_K((r-Pr,\nabla\cdot\Pi\mathbf{e_p})_K-(r-\widehat{Pr},\Pi\mathbf{e_p}\cdot\nu)_{\partial K})+(V(\mathbf{x})(s-s_h),P\mathbf{e}_r)_\Omega\\
&-((s-Ps)_t,P\mathbf{e}_s)_\Omega-(V(\mathbf{x})(r-r_h),P\mathbf{e}_s)_\Omega\\
&-\sum_K((\mathbf{q}-\Pi\mathbf{q},\nabla P\mathbf{e}_s)_K-((\mathbf{q}-\widehat{\Pi\mathbf{q}})\cdot\nu,P\mathbf{e}_s)_{\partial K})-\sum_K((s-Ps,\nabla\cdot\Pi\mathbf{e_q})_K\\
&-(s-\widehat{Ps},\Pi\mathbf{e_q}\cdot\nu)_{\partial K})-(\mathbf{p}-\Pi\mathbf{p},\Pi\mathbf{e_q})_\Omega+(\mathbf{q}-\Pi\mathbf{q},\Pi\mathbf{e_p})_\Omega.
\end{aligned}
$$

By Lemma 2.1 and the Cauchy–Schwarz inequality we get

$$
\frac{1}{2}\frac{d}{dt}\|P\mathbf{e}_r\|_\Omega^2+\frac{1}{2}\frac{d}{dt}\|P\mathbf{e}_s\|_\Omega^2\le Ch^{2k+2}+C_1(\|P\mathbf{e}_r\|_\Omega^2+\|P\mathbf{e}_s\|_\Omega^2+\|\Pi\mathbf{e_p}\|_\Omega^2+\|\Pi\mathbf{e_q}\|_\Omega^2). \tag{3.55}
$$

Finally, integrating the last equation with respect to time between 0 and T, we obtain

$$
\frac{1}{2}(\|P\mathbf{e}_r\|_\Omega^2+\|P\mathbf{e}_s\|_\Omega^2)\le Ch^{2k+2}+C_1\int_0^T(\|P\mathbf{e}_r\|_\Omega^2+\|P\mathbf{e}_s\|_\Omega^2+\|\Pi\mathbf{e_p}\|_\Omega^2+\|\Pi\mathbf{e_q}\|_\Omega^2)dt. \tag{3.56}
$$

3.2.2. The second energy equation

We first take the time derivative in (3.36) and (3.38), and choose the test functions $\omega=(P\mathbf{e}_s)_t$, $\boldsymbol{\eta}=\Pi\mathbf{e_p}$, $\upsilon=(P\mathbf{e}_r)_t$, $\boldsymbol{\xi}=\Pi\mathbf{e_q}$. Then we have

$$
((r-r_h)_t,(P\mathbf{e}_s)_t)_\Omega-B_1(\mathbf{p}-\mathbf{p}_h,s-s_h,(P\mathbf{e}_s)_t)=0, \tag{3.57}
$$

$$
((\mathbf{p}-\mathbf{p}_h)_t,\Pi\mathbf{e_p})_\Omega+B_2((s-s_h)_t,\Pi\mathbf{e_p})=0, \tag{3.58}
$$

$$
((s-s_h)_t,(P\mathbf{e}_r)_t)_\Omega+B_1(\mathbf{q}-\mathbf{q}_h,r-r_h,(P\mathbf{e}_r)_t)=0, \tag{3.59}
$$

$$
((\mathbf{q}-\mathbf{q}_h)_t,\Pi\mathbf{e_q})_\Omega+B_2((r-r_h)_t,\Pi\mathbf{e_q})=0. \tag{3.60}
$$

Summing (3.58)–(3.60) and subtracting (3.57), we obtain

$$
\begin{aligned}
\frac{1}{2}\frac{d}{dt}\|\Pi\mathbf{e_p}\|_\Omega^2+\frac{1}{2}\frac{d}{dt}\|\Pi\mathbf{e_q}\|_\Omega^2=&((r-r_h)_t,(P\mathbf{e}_s)_t)_\Omega-B_1(\mathbf{p}-\mathbf{p}_h,s-s_h,(P\mathbf{e}_s)_t)\\
&-((s-s_h)_t,(P\mathbf{e}_r)_t)_\Omega-B_1(\mathbf{q}-\mathbf{q}_h,r-r_h,(P\mathbf{e}_r)_t)\\
&-((\mathbf{p}-\Pi\mathbf{p})_t,\Pi\mathbf{e_p})_\Omega-B_2((s-s_h)_t,\Pi\mathbf{e_p})\\
&-((\mathbf{q}-\Pi\mathbf{q})_t,\Pi\mathbf{e_q})_\Omega-B_2((r-r_h)_t,\Pi\mathbf{e_q}).
\end{aligned} \tag{3.61}
$$

Similar to (3.54), by the definition of B_1 and B_2 we get

$$
\begin{aligned}
&\frac{1}{2}\frac{d}{dt}\|\Pi\mathbf{e_p}\|_\Omega^2+\frac{1}{2}\frac{d}{dt}\|\Pi\mathbf{e_q}\|_\Omega^2\\
&=((r-Pr)_t,(P\mathbf{e}_s)_t)_\Omega-\sum_K((\mathbf{p}-\Pi\mathbf{p},\nabla(P\mathbf{e}_s)_t)_K-((\mathbf{p}-\widehat{\Pi\mathbf{p}})\cdot\nu,(P\mathbf{e}_s)_t)_{\partial K})\\
&-\sum_K(((s-Ps)_t,\nabla\cdot\Pi\mathbf{e_p})_K-(s_t-\widehat{Ps_t},\Pi\mathbf{e_p}\cdot\nu)_{\partial K})-(V(\mathbf{x})(s-s_h),(P\mathbf{e}_s)_t)_\Omega\\
&-((s-Ps)_t,(P\mathbf{e}_r)_t)_\Omega-(V(\mathbf{x})(r-r_h),(P\mathbf{e}_r)_t)_\Omega\\
&-\sum_K((\mathbf{q}-\Pi\mathbf{q},\nabla(P\mathbf{e}_r)_t)_K-((\mathbf{q}-\widehat{\Pi\mathbf{q}})\cdot\nu,(P\mathbf{e}_r)_t)_{\partial K})-\sum_K(((r-Pr)_t,\nabla\cdot\Pi\mathbf{e_q})_K\\
&-(r_t-\widehat{Pr_t},\Pi\mathbf{e_q}\cdot\nu)_{\partial K})-((\mathbf{p}-\Pi\mathbf{p})_t,\Pi\mathbf{e_p})_\Omega-((\mathbf{q}-\Pi\mathbf{q})_t,\Pi\mathbf{e_q})_\Omega.
\end{aligned}
$$

Integrating it with respect to time t, it follows that

$$
\begin{aligned}
&\frac{1}{2}(\|\Pi\mathbf{e_p}\|_\Omega^2+\|\Pi\mathbf{e_q}\|_\Omega^2)\\
&=\int_0^T-((\mathbf{p}-\Pi\mathbf{p})_t,\Pi\mathbf{e_p})_\Omega-((\mathbf{q}-\Pi\mathbf{q})_t,\Pi\mathbf{e_q})_\Omega dt+\int_0^T((r-Pr)_t,(P\mathbf{e}_s)_t)_\Omega\\
&-((s-Ps)_t,(P\mathbf{e}_r)_t)_\Omega-(V(\mathbf{x})(r-r_h),(P\mathbf{e}_r)_t)_\Omega-(V(\mathbf{x})(s-s_h),(P\mathbf{e}_s)_t)_\Omega dt\\
&-\sum_K\int_0^T((\mathbf{p}-\Pi\mathbf{p},\nabla(P\mathbf{e}_s)_t)_K-((\mathbf{p}-\widehat{\Pi\mathbf{p}})\cdot\nu,(P\mathbf{e}_s)_t)_{\partial K})dt\\
&-\sum_K\int_0^T(((s-Ps)_t,\nabla\cdot\Pi\mathbf{e_p})_K-(s_t-\widehat{Ps_t},\Pi\mathbf{e_p}\cdot\nu)_{\partial K})dt
\end{aligned} \tag{3.62}
$$

$$-\sum_K \int_0^T ((\mathbf{q}-\Pi\mathbf{q}, \nabla(P\mathbf{e}_r)_t)_K - ((\mathbf{q}-\widehat{\Pi\mathbf{q}})\cdot\nu, (P\mathbf{e}_r)_t)_{\partial K})dt$$

$$-\sum_K \int_0^T (((r-Pr)_t, \nabla\cdot\Pi\mathbf{e}_\mathbf{q})_K - (r_t-\widehat{Pr_t}, \Pi\mathbf{e}_\mathbf{q}\cdot\nu)_{\partial K})dt.$$

For the second term we integrate by parts over t and get

$$\int_0^T ((r-Pr)_t, (P\mathbf{e}_s)_t)_\Omega dt = ((r-Pr)_t, P\mathbf{e}_s)_\Omega|_0^t - \int_0^T ((r-Pr)_{tt}, P\mathbf{e}_s)_\Omega dt, \tag{3.63}$$

and

$$\begin{aligned}&\int_0^T (V(\mathbf{x})(r-r_h), (P\mathbf{e}_r)_t)_\Omega dt \\ &= (V(\mathbf{x})(r-r_h), (P\mathbf{e}_r))_\Omega|_0^t - \int_0^T (V(\mathbf{x})(r-Pr)_t, P\mathbf{e}_r)_\Omega dt - \int_0^T (V(\mathbf{x})(P\mathbf{e}_r)_t, P\mathbf{e}_r)_\Omega dt \\ &= (V(\mathbf{x})(r-r_h), (P\mathbf{e}_r))_\Omega|_0^t - \int_0^T (V(\mathbf{x})(r-Pr)_t, P\mathbf{e}_r)_\Omega dt - \frac{1}{2}(V(\mathbf{x})P\mathbf{e}_r, P\mathbf{e}_r)_\Omega|_0^t.\end{aligned} \tag{3.64}$$

Combining (3.62)–(3.64), and using the result in Lemma 2.1 we obtain

$$\begin{aligned}\frac{1}{2}(\|\Pi\mathbf{e}_\mathbf{p}\|_\Omega^2 + \|\Pi\mathbf{e}_\mathbf{q}\|_\Omega^2) \le Ch^{2k+2} + C_2\int_0^T \|P\mathbf{e}_r\|_\Omega^2 + \|P\mathbf{e}_s\|_\Omega^2 + \|\Pi\mathbf{e}_\mathbf{p}\|_\Omega^2 + \|\Pi\mathbf{e}_\mathbf{q}\|_\Omega^2 dt \\ + \widetilde{C}(\|P\mathbf{e}_r\|_\Omega^2 + \|P\mathbf{e}_s\|_\Omega^2).\end{aligned} \tag{3.65}$$

Recalling the first energy equation (3.56), finally we have

$$\frac{1}{2}(\|\Pi\mathbf{e}_\mathbf{p}\|_\Omega^2 + \|\Pi\mathbf{e}_\mathbf{q}\|_\Omega^2) \le Ch^{2k+2} + C_3\int_0^T \|P\mathbf{e}_r\|_\Omega^2 + \|P\mathbf{e}_s\|_\Omega^2 + \|\Pi\mathbf{e}_\mathbf{p}\|_\Omega^2 + \|\Pi\mathbf{e}_\mathbf{q}\|_\Omega^2 dt. \tag{3.66}$$

3.2.3. Proof of the L^2 error estimate

The energy inequalities (3.56) and (3.66) imply that

$$\begin{aligned}\frac{1}{2}(\|\Pi\mathbf{e}_\mathbf{p}\|_\Omega^2 + \|\Pi\mathbf{e}_\mathbf{q}\|_\Omega^2 + \|P\mathbf{e}_r\|_\Omega^2 + \|P\mathbf{e}_s\|_\Omega^2) \le \\ Ch^{2k+2} + C_3\int_0^T \|P\mathbf{e}_r\|_\Omega^2 + \|P\mathbf{e}_s\|_\Omega^2 + \|\Pi\mathbf{e}_\mathbf{p}\|_\Omega^2 + \|\Pi\mathbf{e}_\mathbf{q}\|_\Omega^2 dt.\end{aligned} \tag{3.67}$$

Employing the Gronwall's inequality, we obtain

$$\|\Pi\mathbf{e}_\mathbf{p}\|^2_{L^\infty((0,T);L^2(\Omega))} + \|\Pi\mathbf{e}_\mathbf{q}\|^2_{L^\infty((0,T);L^2(\Omega))} + \|P\mathbf{e}_r\|^2_{L^\infty((0,T);L^2(\Omega))} + \|P\mathbf{e}_s\|^2_{L^\infty((0,T);L^2(\Omega))} \le Ch^{2k+2}. \tag{3.68}$$

After using the projection error estimates, we proved the L^2 error estimate, Theorem 3.1.

4. Negative-order norm error estimate

4.1. Smoothness-increasing accuracy-conserving filter

In order to obtain the superconvergence of LDG methods in negative-order norm over uniform Cartesian mesh, we implement the smoothness-increasing accuracy-conserving (SIAC) filter. The first use of this filter was by Bramble and Schatz [9], Thomée [10] for the continuous finite element methods, Mock and Lax deduced this technique by studying the discontinuous solution of linear hyperbolic equations [11]. Cockburn, Luskin, Shu and Süli [12] initially introduced this technique for discontinuous Galerkin methods that it is feasible to raise the order of accuracy of DG solution from $k+1$ to $2k+1$. Later, this technique was named as a smoothness-increasing accuracy-conserving filter. Assume the DG approximation is given on a uniform Cartesian mesh, the SIAC filter is applied at the final time T and improves the order of accuracy by increasing the smoothness of the solution and reduces the number of oscillations in the error. This is provided by convolving the numerical approximation with the SIAC filter:

$$r_h^* = K_h^{2k+1,k+1} * r_h,$$

where r_h^* is the filtered solution, r_h is the DG solution calculated at the final time T, and $K_h^{2k+1,k+1}(\boldsymbol{x}) = K^{2k+1,k+1}(\boldsymbol{x}/h)/h^d$ is the symmetric SIAC filter. The kernel $K^{2k+1,k+1}$ has compact support and translation-invariant, and it is composed of a linear combination of B-splines of order $k+1$ obtained by convolving the characteristic function over the interval $(-\frac{1}{2}, \frac{1}{2})$ with

itself k times, scaled by the uniform mesh size. Let χ be the characteristic function of the interval $(-\frac{1}{2}, \frac{1}{2})$ and let δ denote the Dirac distribution connected at $x = 0$, then we define recursively the functions ψ^i as

$$\psi^0 = \delta, \qquad \psi^{k+1} = \psi^k * \chi,$$

and the one-dimensional convolution kernel is of the form

$$K_h^{2k+1,k+1}(x) = \frac{1}{h}\sum_{\gamma=-k}^{k} c_\lambda^{2k+1,k+1}\psi^{k+1}(\frac{x}{h} - \gamma). \tag{4.69}$$

Given an arbitrary $\mathbf{x} = (x_1, \ldots, x_d) \in R^d$, the kernel for the multi-dimensional space is of the form

$$K_h^{2k+1,k+1}(\boldsymbol{x}) = \sum_{\gamma\in Z^d} c_\lambda^{2k+1,k+1}\psi^{k+1}(\boldsymbol{x} - \gamma), \tag{4.70}$$

where

$$\psi^{k+1}(\boldsymbol{x}) = \psi^{k+1}(x_1)\cdots\psi^{k+1}(x_d).$$

The coefficients $c_\gamma^{2k+1,k+1}$ are tensor products of the one-dimensional coefficient. These one-dimensional coefficients are chosen such that $K^{2(k+1),k+1} * p = p$ for polynomials p of degree $2k$. The following notation for the difference quotients over element of size h is used:

$$\partial_{h,j}v(\mathbf{x}) = \frac{1}{h}(v(\mathbf{x} + \frac{1}{2}he_j) - v(\mathbf{x} - \frac{1}{2}he_j)),$$

here e_j is the unit multi-index whose jth component is 1 and others 0. For any multi-index $\alpha = (\alpha_1, \ldots, \alpha_d)$ we set αth-order difference quotient to be

$$\partial_h^\alpha v(\mathbf{x}) = (\partial_{h,1}^{\alpha_1}, \ldots, \partial_{h,d}^{\alpha_d})v(\mathbf{x}).$$

Theorem 4.1 (*Bramble and Schatz [9]*). *For $0 < T < T^*$, where T^* is the maximal time of the existence of classical solutions, let $u \in L^\infty((0,T); H^{2k+2}(\Omega)) \cap L^2((0,T); H^{2k+2}(\Omega))$ be the exact solution of the problem (1.1). Let U be any approximation to u, and $\Omega_0 + 2supp(K^{2k+1,k+1}(x)) \subset\subset \Omega$ then*

$$\|u(T) - K_h^{2(k+1),k+1} * U\|_{0,\Omega_0} \le \frac{h^{2k+1}}{(2k+2)!}C_1|u|_{2k+2,\Omega} + C_2\sum_{|\alpha|\le k+1}\|\partial_h^\alpha(u-U)\|_{-(k+1),\Omega},$$

where C_1 and C_2 depend solely on Ω_0, Ω_1, d, k, $c_\gamma^{2k+1,k+1}$ and are independent of h.

Remark 4.1. For our problem we only consider periodic boundary conditions and we take $U = u_h$ represent the LDG approximation. We obtain the estimate for the entire domain, i.e., $\Omega_0 = \Omega$ by considering $\Omega\backslash\Omega_0$ as the interior part of a new period of the domain.

We neglect to provide the details of this proof, which is shown in [9] and [12], as well as that of Ryan and Cockburn [23] and Thomée [10]. The goal of this section is to demonstrate that the higher-order convergence in the negative-order norm can be obtained for variable coefficient Schrödinger equations. We give our main result as follows:

Theorem 4.2. *For $0 < T < T^*$ where T^* is the maximal time of the classical solutions, let r, s be the exact solutions of the problem (3.16) and (3.17) subject to smooth initial and periodic boundary conditions, r, $s \in L^\infty([0,T]; W^{\infty,2k+2}(\Omega)) \cap L^\infty([0,T]; H^{2k+2}(\Omega)) \cap L^2((0,T); H^{k+2}(\Omega))$ and $V(x)$ be smooth, if r_h and s_h are solutions to (3.23) and (3.25) then*

$$\|r(T) - r_h(T)\|_{-(k+1),\Omega} \le Ch^{2k}, \tag{4.71}$$

$$\|s(T) - s_h(T)\|_{-(k+1),\Omega} \le Ch^{2k}, \tag{4.72}$$

where C is a constant independent of h and depends on $\|r_0\|_{-(k+1),\Omega}$, $\|s_0\|_{-(k+1),\Omega}$ and T.

Remark 4.2. In Theorem 4.2 we prove the negative-order norm estimate for the variable coefficient Schrödinger equations, but in the numerical tests we can also obtain the same results for the nonlinear Schrödinger equations. However, the theoretic proof is not trivial. We leave it for the future work.

Remark 4.3. As noted in [12], because the spatial derivative term is linear in (1.1), then we have

$$\|\partial_h^\alpha(r - r_h)\|_{-l,\Omega} \le C\|\partial_h^\alpha r_0\|_{l,\Omega}h^{2k},$$

$$\|\partial_h^\alpha(s - s_h)\|_{-l,\Omega} \le C\|\partial_h^\alpha s_0\|_{l,\Omega}h^{2k},$$

therefore, as long as this increase in accuracy can be demonstrated in the negative-order norm, then we have $\mathbb{O}(h^{2k})$ accuracy for the post-processed solution in the L^2-norm.

Theorem 4.3. *Let r, s be the exact solutions of the problem (3.16) and (3.17), r_h and s_h be the approximate solutions that satisfy the scheme (3.23)–(3.26). Let $K_h^{2k+1,k+1}$ be a SIAC filter (4.70). Assuming that the initial data r_0 and s_0 are smooth enough, then we obtain the error estimates,*

$$\|r - K_h^{2k+1,k+1} * r_h\|_\Omega \le Ch^{2k},$$

$$\|s - K_h^{2k+1,k+1} * s_h\|_\Omega \le Ch^{2k},$$

and C is dependent on u_0, T and independent of h.

It can be obtained by combining Theorems 4.1, 4.2 as well as Remark 4.3. Next we will give details of the proof for Theorem 4.2.

4.2. Negative-order norm error estimates

In order to extract the hidden accuracy in the LDG solution, we need to estimate the negative-order norm

$$\|r(T) - r_h(T)\|_{-l,\Omega} = \sup_{\Phi\in C_0^\infty} \frac{(r(T) - r_h(T), \Phi)_\Omega}{\|\Phi\|_{l,\Omega}}, \quad l \ge 0, \tag{4.73}$$

$$\|s(T) - s_h(T)\|_{-l,\Omega} = \sup_{\Psi\in C_0^\infty} \frac{(s(T) - s_h(T), \Psi)_\Omega}{\|\Psi\|_{l,\Omega}}, \quad l \ge 0, \tag{4.74}$$

so we need to analyze the inner products

$$(r(T) - r_h(T), \Phi)_\Omega \qquad \text{and} \qquad (s(T) - s_h(T), \Psi)_\Omega.$$

Estimating the inner products requires considering the dual equations to (3.16) and (3.17). The dual equations are not uniquely defined, so we have freedom to choose the dual equations. Here we choose the dual equations of the form: find functions φ and ψ such that $\varphi(\cdot, t)$ and $\psi(\cdot, t)$ are one-periodic for all $t \in [0, T]$ and

$$\varphi_t + \Delta\psi - V(\mathbf{x})\psi = 0, \quad (x, t) \in \Omega \times (0, T], \tag{4.75}$$

$$\psi_t - \Delta\varphi + V(\mathbf{x})\varphi = 0, \quad (x, t) \in \Omega \times (0, T], \tag{4.76}$$

where

$$\varphi(x, T) = \frac{\Phi(x)}{\|\Phi\|_{k+1,\Omega}}, \qquad \psi(x, T) = \frac{\Psi(x)}{\|\Psi\|_{k+1,\Omega}}. \tag{4.77}$$

We multiply (3.16) by φ and (3.17) by ψ, and for the dual equations we multiply (4.75) by r and multiply (4.76) by s. Then after integrating it over Ω, we obtain

$$\begin{aligned} 0 &= \frac{d}{dt}((r, \varphi)_\Omega + (s, \psi)_\Omega) \\ &= (r_t, \varphi)_\Omega + (r, \varphi_t)_\Omega + (s_t, \psi)_\Omega + (s, \psi_t)_\Omega \\ &= (-\Delta s + V(\boldsymbol{x})s, \varphi)_\Omega + (r, -\Delta\psi + V(\mathbf{x})\psi)_\Omega + (\Delta r - V(\boldsymbol{x})r, \psi)_\Omega + (s, \Delta\varphi - V(\mathbf{x})\varphi)_\Omega. \end{aligned} \tag{4.78}$$

This relation allows us to estimate the terms $(r(T) - r_h(T), \Phi)_\Omega$ and $(s(T) - s_h(T), \Psi)_\Omega$ appearing in the definition of the negative norm (4.73) and (4.74). That is

$$\begin{aligned} &\frac{(r(T) - r_h(T), \Phi)_\Omega}{\|\Phi\|_{k+1,\Omega}} + \frac{(s(T) - s_h(T), \Psi)_\Omega}{\|\Psi\|_{k+1,\Omega}} \\ &= (r(0) - r_h(0), \varphi(0))_\Omega + (s(0) - s_h(0), \psi(0))_\Omega + \int_0^T \frac{d}{dt}((r - r_h, \varphi)_\Omega + (s - s_h, \psi)_\Omega)dt \\ &= (r(0) - r_h(0), \varphi(0))_\Omega + (s(0) - s_h(0), \psi(0))_\Omega - \int_0^T \frac{d}{dt}((r_h, \varphi)_\Omega + (s_h, \psi)_\Omega)dt. \end{aligned}$$

For any functions $\chi, \omega \in V_h$, we have

$$\begin{aligned}
&\frac{d}{dt}((r_h, \varphi)_\Omega + (s_h, \psi)_\Omega) \\
&= ((r_h)_t, \varphi)_\Omega + (r_h, \varphi_t)_\Omega + ((s_h)_t, \psi)_\Omega + (s_h, \psi_t)_\Omega \\
&= ((r_h)_t, \varphi - \chi)_\Omega - B_1(\mathbf{p}_h, s_h, \varphi - \chi) + B_1(\mathbf{p}_h, s_h, \varphi) + (r_h, \varphi_t)_\Omega \\
&\quad ((s_h)_t, \psi - \omega)_\Omega + B_1(\mathbf{q}_h, r_h, \psi - \omega) - B_1(\mathbf{q}_h, r_h, \psi) + (s_h, \psi_t)_\Omega.
\end{aligned}$$

By the definition of B_1 we have

$$\begin{aligned}
B_1(\mathbf{p}_h, s_h, \varphi) + (s_h, \psi_t)_\Omega &= (\mathbf{p}_h, \nabla\varphi)_\Omega + (V(\mathbf{x})s_h, \varphi)_\Omega - \sum_K (\widehat{\mathbf{p}_h} \cdot \nu, \varphi)_{\partial K} + (s_h, \psi_t)_\Omega \\
&= (\mathbf{p}_h, \nabla\varphi)_\Omega + (V(\mathbf{x})s_h, \varphi)_\Omega + (s_h, \Delta\varphi - V(\mathbf{x})\varphi)_\Omega \\
&= (\mathbf{p}_h, \nabla\varphi)_\Omega + (s_h, \Delta\varphi)_\Omega,
\end{aligned}$$

where in the second equality we use the continuity of the φ and the periodic boundary conditions, and in the last equality we use the definition of the dual problem (4.76). Similarly we also have

$$-B_1(\mathbf{q}_h, r_h, \psi) + (r_h, \varphi_t)_\Omega = -(\mathbf{q}_h, \nabla\psi)_\Omega - (r_h, \Delta\psi)_\Omega.$$

Combining the above, we have

$$\begin{aligned}
&\frac{(r(T) - r_h(T), \Phi)_\Omega}{\|\Phi\|_{k+1,\Omega}} + \frac{(s(T) - s_h(T), \Psi)_\Omega}{\|\Psi\|_{k+1,\Omega}} \\
&= (r(0) - r_h(0), \varphi(0))_\Omega + (s(0) - s_h(0), \psi(0))_\Omega - \int_0^T ((r_h)_t, \varphi - \chi)_\Omega - B_1(\mathbf{p}_h, s_h, \varphi - \chi) \\
&\quad + ((s_h)_t, \psi - \omega)_\Omega + B_1(\mathbf{q}_h, r_h, \psi - \omega)dt - \int_0^T (\mathbf{p}_h, \nabla\varphi)_\Omega + (s_h, \Delta\varphi)_\Omega - (\mathbf{q}_h, \nabla\psi)_\Omega - (r_h, \Delta\psi)_\Omega dt \\
&= \Theta_1 + \Theta_2 + \Theta_3,
\end{aligned}$$

where

$$\begin{aligned}
\Theta_1 &= (r(0) - r_h(0), \varphi(0))_\Omega + (s(0) - s_h(0), \psi(0))_\Omega, \\
\Theta_2 &= -\int_0^T ((r_h)_t, \varphi - \chi)_\Omega - B_1(\mathbf{p}_h, s_h, \varphi - \chi) + ((s_h)_t, \psi - \omega)_\Omega + B_1(\mathbf{q}_h, r_h, \psi - \omega)dt, \\
\Theta_3 &= -\int_0^T (\mathbf{p}_h, \nabla\varphi)_\Omega + (s_h, \Delta\varphi)_\Omega - (\mathbf{q}_h, \nabla\psi)_\Omega - (r_h, \Delta\psi)_\Omega dt.
\end{aligned}$$

Lemma 4.4 (*Estimating the First Term*)**.** *There exists a positive constant $\widetilde{C}_1$, independent of h, such that*

$$|\Theta_1| \le \widetilde{C}_1 h^{2k+1}\|r_0\|_{k+1,\Omega}\|\varphi(0)\|_{k+1,\Omega} + \widetilde{C}_1 h^{2k+1}\|s_0\|_{k+1,\Omega}\|\psi(0)\|_{k+1,\Omega}. \tag{4.79}$$

We neglect to provide a proof of this lemma as it can easily be obtained by using the property of the projections for initial conditions. For the second term Θ_2, we have the following result:

Lemma 4.5 (*Estimate the Second Term*)**.** *There exists a positive constant $\widetilde{C}_2$, independent of h, such that*

$$\begin{aligned}
|\Theta_{21}| \le& \widetilde{C}_2 h^{k+1}\Big(\int_0^T \|r - r_h\|_\Omega^2 dt\Big)^{\frac{1}{2}}\Big(\int_0^T \|\varphi\|_{k+1,\Omega}^2 dt\Big)^{\frac{1}{2}} + \widetilde{C}_2 h^{2k+2}\Big(\int_0^T \|\varphi\|_{k+1,\Omega}^2 dt\Big)^{\frac{1}{2}} \\
&+ \widetilde{C}_2 h^{2k+1}\Big(\int_0^T \|\varphi\|_{k+1,\Omega}^2 dt\Big)^{\frac{1}{2}} + \widetilde{C}_2 h^{k}\Big(\int_0^T \|\mathbf{p} - \mathbf{p}_h\|_\Omega^2 dt\Big)^{\frac{1}{2}}\Big(\int_0^T \|\varphi\|_{k+1,\Omega}^2 dt\Big)^{\frac{1}{2}},
\end{aligned} \tag{4.80}$$

and

$$\begin{aligned}
|\Theta_{22}| \le& \widetilde{C}_2 h^{k+1}\Big(\int_0^T \|s - s_h\|_\Omega^2 dt\Big)^{\frac{1}{2}}\Big(\int_0^T \|\psi\|_{k+1,\Omega}^2 dt\Big)^{\frac{1}{2}} + \widetilde{C}_2 h^{2k+2}\Big(\int_0^T \|\psi\|_{k+1,\Omega}^2 dt\Big)^{\frac{1}{2}} \\
&+ \widetilde{C}_2 h^{2k+1}\Big(\int_0^T \|\psi\|_{k+1,\Omega}^2 dt\Big)^{\frac{1}{2}} + \widetilde{C}_2 h^{k}\Big(\int_0^T \|\mathbf{q} - \mathbf{q}_h\|_\Omega^2 dt\Big)^{\frac{1}{2}}\Big(\int_0^T \|\psi\|_{k+1,\Omega}^2 dt\Big)^{\frac{1}{2}},
\end{aligned} \tag{4.81}$$

where

$$\Theta_{21} = -\int_0^T ((r_h)_t, \varphi - \chi)_\Omega - B_1(\mathbf{p}_h, s_h, \varphi - \chi)dt, \tag{4.82}$$

$$\Theta_{22} = -\int_0^T ((s_h)_t, \psi - \omega)_\Omega + B_1(\mathbf{q}_h, r_h, \psi - \omega)dt. \tag{4.83}$$

Proof. Firstly by the definition of (4.82) for Θ_{21}, we consider the terms insider the integral and let $\chi = P\varphi$. Here we use the standard L^2-projections $P = P_k$, $\Pi = \Pi_k$. This gives

$$((r_h)_t, \varphi - P\varphi)_\Omega = 0, \tag{4.84}$$

and reduces the terms inside the integral to the following:

$$\begin{aligned}
&B_1(\mathbf{p}_h, s_h, \varphi - P\varphi)\\
=&(\mathbf{p}_h, \nabla(\varphi - P\varphi))_\Omega + (V(\mathbf{x})s_h, \varphi - P\varphi)_\Omega - \sum_K (\widehat{\mathbf{p}}_h \cdot \nu, \varphi - P\varphi)_{\partial K}\\
=&-(\nabla \cdot \mathbf{p}_h, \varphi - P\varphi)_\Omega + (V(\mathbf{x})s_h, \varphi - P\varphi)_\Omega + \sum_K ((\mathbf{p}_h - \widehat{\mathbf{p}}_h) \cdot \nu, \varphi - P\varphi)_{\partial K}\\
=&(V(x)s_h, \varphi - P\varphi)_\Omega + \sum_K ((\mathbf{p}_h - \widehat{\mathbf{p}}_h) \cdot \nu, \varphi - P\varphi)_{\partial K}\\
=&(V(\mathbf{x})(s_h - s), \varphi - P\varphi)_\Omega + (V(\mathbf{x})s - P(V(\mathbf{x})s), \varphi - P\varphi)_\Omega\\
&+ \sum_K ((\mathbf{p}_h - \widehat{\mathbf{p}}_h) \cdot \nu, \varphi - P\varphi)_{\partial K}\\
=&(I) + (II) + (III).
\end{aligned}$$

Now we define

$$\begin{aligned}
(I) &= (V(\mathbf{x})(s_h - s), \varphi - P\varphi)_\Omega,\\
(II) &= (V(\mathbf{x})s - P(V(\mathbf{x})s), \varphi - P\varphi)_\Omega,\\
(III) &= \sum_K ((\mathbf{p}_h - \widehat{\mathbf{p}}_h) \cdot \nu, \varphi - P\varphi)_{\partial K}.
\end{aligned}$$

Using the boundedness of $V(\mathbf{x})$ and Cauchy–Schwarz inequality, we have the following estimates.
Estimate of (I):

$$|(I)| \le C\|s - s_h\|_\Omega \|\varphi - P\varphi\|_\Omega.$$

Estimate of (II):

$$|(II)| \le C\|V(\mathbf{x})s - P(V(\mathbf{x})s)\|_\Omega \|\varphi - P\varphi\|_\Omega.$$

Estimate of (III):
For this estimate we use the Lipschitz continuity of $\widehat{f}$ and the inverse inequality and obtain:

$$\begin{aligned}
|(III)| =& \sum_K ((\mathbf{p}_h - \mathbf{p} + \mathbf{p} - \widehat{\mathbf{p}}_h) \cdot \nu, \varphi - P\varphi)_{\partial K}\\
\le& C \sum_K \int_{\partial K} |\mathbf{p} - \mathbf{p}_h||\varphi - P\varphi| ds\\
\le& C\|\mathbf{p} - \mathbf{p}_h\|_\Gamma \|\varphi - P\varphi\|_\Gamma\\
\le& Ch^{k+\frac{1}{2}} \|\mathbf{p} - \mathbf{p}_h\|_\Gamma \|\varphi\|_{k+1,\Omega}\\
=& Ch^{k+\frac{1}{2}} \|\mathbf{p} - \Pi\mathbf{p} + \Pi\mathbf{p} - \mathbf{p}_h\|_\Gamma \|\varphi\|_{k+1,\Omega}\\
\le& Ch^k \|\mathbf{p} - \mathbf{p}_h\|_\Omega \|\varphi\|_{k+1,\Omega} + Ch^{2k+1} \|\varphi\|_{k+1,\Omega}.
\end{aligned}$$

We can combine these estimates to estimate the second term Θ_{21}:

$$\begin{aligned}
|\Theta_{21}| \le& C \int_0^T (I + II + III)\\
\le& \widetilde{C}_2 h^{k+1} \Big(\int_0^T \|s - s_h\|_\Omega^2 dt\Big)^{\frac{1}{2}} \Big(\int_0^T \|\varphi\|_{k+1,\Omega}^2 dt\Big)^{\frac{1}{2}} + \widetilde{C}_2 h^{2k+2} \Big(\int_0^T \|\varphi\|_{k+1,\Omega}^2 dt\Big)^{\frac{1}{2}}\\
&+ \widetilde{C}_2 h^{2k+1} \Big(\int_0^T \|\varphi\|_{k+1,\Omega}^2 dt\Big)^{\frac{1}{2}} + \widetilde{C}_2 h^k \Big(\int_0^T \|\mathbf{p} - \mathbf{p}_h\|_\Omega^2 dt\Big)^{\frac{1}{2}} \Big(\int_0^T \|\varphi\|_{k+1,\Omega}^2 dt\Big)^{\frac{1}{2}}.
\end{aligned}$$

Similar to Θ_{21}, we have

$$|\Theta_{22}| \leq \widetilde{C}_2 h^{k+1}\Big(\int_0^T \|s-s_h\|_\Omega^2 dt\Big)^{\frac{1}{2}}\Big(\int_0^T \|\psi\|_{k+1,\Omega}^2 dt\Big)^{\frac{1}{2}} + \widetilde{C}_2 h^{2k+2}\Big(\int_0^T \|\psi\|_{k+1,\Omega}^2 dt\Big)^{\frac{1}{2}}$$
$$+ \widetilde{C}_2 h^{2k+1}\Big(\int_0^T \|\psi\|_{k+1,\Omega}^2 dt\Big)^{\frac{1}{2}} + \widetilde{C}_2 h^{k}\Big(\int_0^T \|\mathbf{q}-\mathbf{q}_h\|_\Omega^2 dt\Big)^{\frac{1}{2}}\Big(\int_0^T \|\psi\|_{k+1,\Omega}^2 dt\Big)^{\frac{1}{2}}.$$

Next, we need to estimate the third term Θ_3.

Lemma 4.6 (*Estimating the Third Term*)**.** *There exists a positive constant $\widetilde{C}_3$, independent of h, such that*

$$|\Theta_{31}| \leq \widetilde{C}_3\Big(h^k \int_0^T \|\mathbf{p}-\mathbf{p}_h\|_\Omega^2 dt\Big)^{\frac{1}{2}} + h^{k-1}\Big(\Big(\int_0^T \|s-s_h\|_\Omega^2 dt\Big)^{\frac{1}{2}}\Big)\Big(\int_0^T \|\varphi\|_{k+1,\Omega}^2 dt\Big)^{\frac{1}{2}},$$
$$|\Theta_{32}| \leq \widetilde{C}_3\Big(h^k \int_0^T \|\mathbf{q}-\mathbf{q}_h\|_\Omega^2 dt\Big)^{\frac{1}{2}} + h^{k-1}\Big(\Big(\int_0^T \|r-r_h\|_\Omega^2 dt\Big)^{\frac{1}{2}}\Big)\Big(\int_0^T \|\psi\|_{k+1,\Omega}^2 dt\Big)^{\frac{1}{2}},$$

where

$$\Theta_{31} = -\int_0^T (\mathbf{p}_h, \nabla\varphi)_\Omega + (s_h, \Delta\varphi)_\Omega dt,$$
$$\Theta_{32} = \int_0^T (\mathbf{q}_h, \nabla\psi)_\Omega + (r_h, \Delta\psi)_\Omega dt.$$

Proof. Recall the definitions of Θ_{31} and B_2, and the same as Lemma 4.5 we take the standard L^2-projection $P = P_k$. Thus,

$$\begin{aligned}\Theta_{31} &= -\int_0^T (\mathbf{p}_h, \nabla\varphi)_\Omega + (s_h, \Delta\varphi)_\Omega dt\\ &= -\int_0^T (\mathbf{p}_h, \nabla\varphi - \nabla(P\varphi))_\Omega + B_2(s_h, \nabla\varphi - \nabla(P\varphi))dt.\end{aligned}$$

We denote the terms inside the integral of Θ_{31}

$$\begin{aligned}(IV) =&(\mathbf{p}_h, \nabla\varphi - \nabla(P\varphi))_\Omega + B_2(s_h, \nabla\varphi - \nabla(P\varphi))\\ =&(\mathbf{p}_h, \nabla\varphi - \nabla(P\varphi))_\Omega + (s_h, \nabla\cdot(\nabla\varphi - \nabla(P\varphi)))_\Omega - \sum_K (\widehat{s_h}, (\nabla\varphi - \nabla(P\varphi))\cdot\nu)_{\partial K}\\ =&(\mathbf{p}_h, \nabla\varphi - \nabla(P\varphi))_\Omega - (\nabla(s_h), \nabla\varphi - \nabla(P\varphi))_\Omega + \sum_K ((s_h - \widehat{s_h}), (\nabla\varphi - \nabla(P\varphi))\cdot\nu)_{\partial K}.\end{aligned}$$

Because $\nabla s = \mathbf{p}$, so we have

$$\begin{aligned}(IV) =&(\mathbf{p}_h - \mathbf{p}, \nabla\varphi - \nabla(P\varphi))_\Omega + \sum_K ((s_h - \widehat{s_h}), (\nabla\varphi - \nabla(P\varphi))\cdot\nu)_{\partial K}\\ &+ (\nabla(s - s_h), \nabla\varphi - \nabla(P\varphi))_\Omega\\ =&(\mathbf{p}_h - \mathbf{p}, \nabla\varphi - \nabla(P\varphi))_\Omega + \sum_K ((s - \widehat{s_h}), (\nabla\varphi - \nabla(P\varphi))\cdot\nu)_{\partial K}\\ &- (s - s_h, \Delta\varphi - \Delta P\varphi)_\Omega\\ =&(\mathbf{p}_h - \mathbf{p}, \nabla\varphi - \nabla(P\varphi))_\Omega + \sum_K ((s - \widehat{s_h}), (\nabla\varphi - \nabla(P\varphi))\cdot\nu)_{\partial K}\\ &- (s - s_h, \Delta\varphi - \Delta P\varphi)_\Omega.\end{aligned}$$

Then, it follows that

$$|(IV)| \leq Ch^{-1}\|\mathbf{p}-\mathbf{p}_h\|_\Omega\|\varphi - P\varphi\|_\Omega + Ch^{-2}\|s-s_h\|_\Omega\|\varphi - P\varphi\|_\Omega.$$

Therefore, we get

$$|\Theta_{31}| \leq \widetilde{C}_3\Big(h^k \int_0^T \|\mathbf{p}-\mathbf{p}_h\|_\Omega^2 dt\Big)^{\frac{1}{2}} + h^{k-1}\Big(\Big(\int_0^T \|s-s_h\|_\Omega^2 dt\Big)^{\frac{1}{2}}\Big)\Big(\int_0^T \|\varphi\|_{k+1,\Omega}^2 dt\Big)^{\frac{1}{2}}.$$

Similarly,

$$|\Theta_{32}| \leq \widetilde{C}_3\Big(h^k \int_0^T \|\mathbf{q}-\mathbf{q}_h\|_\Omega^2 dt\Big)^{\frac{1}{2}} + h^{k-1}\Big(\Big(\int_0^T \|r-r_h\|_\Omega^2 dt\Big)^{\frac{1}{2}}\Big)\Big(\int_0^T \|\psi\|_{k+1,\Omega}^2 dt\Big)^{\frac{1}{2}}. \quad \square$$

Combining Lemmas 4.4–4.6, we can estimate the numerator in the negative-norm:

$$\begin{aligned}
&\frac{(r(T)-r_h(T),\Phi)_\Omega}{\|\Phi\|_{k+1,\Omega}}+\frac{(s(T)-s_h(T),\Psi)_\Omega}{\|\Psi\|_{k+1,\Omega}}\\
=&\Theta_1+\Theta_{21}+\Theta_{22}+\Theta_{31}+\Theta_{32}\\
\le&Ch^{2k+1}\|\varphi(0)\|_{k+1,\Omega}+Ch^{2k+2}(\int_0^T\|\varphi\|^2_{k+1,\Omega}dt)^{\frac12}+Ch^{2k+2}(\int_0^T\|\varphi\|^2_{k+1,\Omega}dt)^{\frac12}\\
&+Ch^{2k+1}(\int_0^T\|\varphi\|^2_{k+1,\Omega}dt)^{\frac12}+Ch^{2k}(\int_0^T\|\varphi\|^2_{k+1,\Omega}dt)^{\frac12}+Ch^{2k+2}(\int_0^T\|\varphi\|^2_{k+1,\Omega}dt)^{\frac12}\\
&+Ch^{2k+1}\|\psi(0)\|_{k+1,\Omega}+Ch^{2k+2}(\int_0^T\|\psi\|^2_{k+1,\Omega}dt)^{\frac12}+Ch^{2k+2}(\int_0^T\|\psi\|^2_{k+1,\Omega}dt)^{\frac12}\\
&+Ch^{2k+1}(\int_0^T\|\psi\|^2_{k+1,\Omega}dt)^{\frac12}+Ch^{2k}(\int_0^T\|\psi\|^2_{k+1,\Omega}dt)^{\frac12}+Ch^{2k}(\int_0^T\|\psi\|^2_{k+1,\Omega}dt)^{\frac12}.
\end{aligned}$$

It is easy to convert the final time dual problem to an initial problem by changing the time $t'=T-t$ then we have

$$\|\varphi\|_{k+1,\Omega}\le C\|\varphi(T)\|_{k+1,\Omega}\qquad\text{and}\qquad\|\psi\|_{k+1,\Omega}\le C\|\psi(T)\|_{k+1,\Omega}.$$

Therefore we have the estimate for the negative-order norm given by

$$\begin{aligned}
&\|r(T)-r_h(T)\|_{-k+1,\Omega}+\|s(T)-s_h(T)\|_{-k+1,\Omega}\\
=&\sup_{\Phi\in C_0^\infty}\frac{(r(T)-r_h(T),\Phi)_\Omega}{\|\Phi\|_{k+1,\Omega}}+\sup_{\Psi\in C_0^\infty}\frac{(s(T)-s_h(T),\Psi)_\Omega}{\|\Psi\|_{k+1,\Omega}}\\
\le&Ch^s,
\end{aligned}$$

where $s=2k$.

5. Numerical studies

In this section, we present numerical results confirming that the convergence rate of the LDG solutions to Schrödinger equations, and we can improve it from $\mathcal{O}(h^{k+1})$ to $\mathcal{O}(h^{2k+1})$ numerically through the use of the SIAC filter. Firstly we consider the one-dimensional linear Schrödinger equation and the equation including a potential term in the second example. Then we also consider the nonlinear Schrödinger equation where the nonlinear term is given by $f(u)=2|u|^2$. In the final example we consider the LDG solutions for the two-dimensional Schrödinger equation by using a tensor-product polynomial $\mathcal{Q}^k$ approximation space. All the examples are calculated by using LDG method with the alternating flux on the uniform Cartesian mesh as in [25]. In each example, the error is computed using six-point Gauss quadrature rule, and we can clearly see that we get at least $\mathcal{O}(h^{2k+1})$ accuracy after post-processing.

We note that the theoretical estimates presented hold for the uniform mesh assumption, however, in [17,18] it was demonstrated that high-order information can also be extracted over nonuniform and unstructured mesh.

Example 5.1. We begin by presenting the linear Schrödinger equation with a smooth solution in the domain $\Omega=[0,2\pi]$:

$$\begin{aligned}
&iu_t+u_{xx}=0,\quad \Omega\times(0,T),\\
&u(x,0)=\cos(x)+i\sin(x),\quad x\in\Omega,
\end{aligned}$$

with periodic boundary conditions.

The errors and convergence rates are presented in Table 5.1, Figs. 5.1, 5.2 and computed at time $T=6$. In Table 5.1, we show the L^2 and L^∞ errors and convergence rates for this problem before and after the post-processing. Even though Theorem 4.3 only guarantees $\mathcal{O}(h^{2k})$ superconvergence, we can clearly see that the order of accuracy $\mathcal{O}(h^{k+1})$ before the post-processing and at least $\mathcal{O}(h^{2k+1})$ after the post-processing for P^k-elements in both the L^2 and L^∞ norms. In Fig. 5.1 we plot the errors of the numerical solutions before and after post-processing for P^2 and P^3 with 20 uniform elements. It shows that the errors before post-processing are highly oscillatory, and the post-processing gets rid of the oscillatory in the error and greatly reduces its magnitude. In Fig. 5.2, we plot the logarithmic scale of the absolute errors before and after post-processing. Similarly we see that the post-processed errors are less oscillatory and much smaller in magnitude.

Example 5.2. In this example, we consider a classic problem which includes a potential corresponding to a Harmonic oscillator,

$$iu_t+u_{xx}-V(x)u=0,\quad \Omega\times(0,T),$$

Table 5.1
L^2- and L^∞-errors of real part and imaginary part of the linear Schrödinger equation in Example 5.1, before and after post-processing at time $T = 6$ using LDG method.

		Real part before post-processing				Real part after post-processing			
	N	L^2 error	Order	L^∞ error	Order	L^2 error	Order	L^∞ error	Order
P^1	10	2.18E−02	–	7.54E−02	–	2.04E−03	–	3.04E−03	–
	20	4.56E−03	2.26	1.64E−02	2.20	1.28E−04	4.00	1.92E−04	3.98
	40	1.14E−03	2.01	4.11E−03	2.00	7.99E−06	4.00	1.21E−05	3.99
	80	2.84E−04	2.00	1.03E−03	2.00	4.99E−07	4.00	7.57E−07	4.00
	160	7.09E−05	2.00	2.57E−04	2.00	3.12E−08	4.00	4.74E−08	4.00
P^2	10	8.09E−04	–	2.87E−03	–	1.36E−04	–	1.90E−04	–
	20	1.17E−04	2.79	4.99E−04	2.52	2.24E−06	5.92	3.19E−06	5.90
	40	1.51E−05	2.96	6.46E−05	2.95	3.55E−08	5.98	5.06E−08	5.98
	80	1.88E−06	3.00	8.07E−06	3.00	5.57E−10	5.99	7.93E−10	5.99
	160	2.36E−07	3.00	1.01E−06	3.00	8.71E−12	6.00	1.24E−11	6.00
P^3	10	3.53E−05	–	1.21E−04	–	1.61E−05	–	2.28E−05	–
	20	2.92E−06	3.60	1.29E−05	3.24	6.88E−08	7.87	9.73E−08	7.87
	40	1.91E−07	3.93	9.39E−07	3.78	2.75E−10	7.97	3.89E−10	7.97
	80	1.17E−08	4.01	5.10E−08	4.20	1.08E−12	7.99	1.53E−12	7.99
	160	6.60E−10	4.11	3.16E−09	4.01	4.30E−15	7.97	6.08E−15	7.97
		Imaginary part before post-processing				Imaginary part after post-processing			
	N	L^2 error	Order	L^∞ error	Order	L^2 error	Order	L^∞ error	Order
P^1	10	2.18E−02	–	7.22E−02	–	2.04E−03	–	3.04E−03	–
	20	4.56E−03	2.26	1.64E−02	2.12	1.28E−04	4.00	1.92E−04	3.98
	40	1.14E−03	2.01	4.11E−03	2.00	7.99E−06	4.00	1.21E−05	3.99
	80	2.84E−04	2.00	1.03E−03	2.00	4.99E−07	4.00	7.57E−07	4.00
	160	7.09E−05	2.00	2.57E−04	2.00	3.12E−08	4.00	4.74E−08	4.00
P^2	10	8.09E−04	–	2.73E−03	–	1.36E−04	–	1.93E−04	–
	20	1.17E−04	2.79	4.99E−04	2.45	2.24E−06	5.92	3.19E−06	5.92
	40	1.51E−05	2.96	6.46E−05	2.95	3.55E−08	5.98	5.06E−08	5.98
	80	1.88E−06	3.00	8.07E−06	3.00	5.57E−10	5.99	7.93E−10	6.00
	160	2.36E−07	3.00	1.01E−06	3.00	8.71E−12	6.00	1.24E−11	6.00
P^3	10	3.53E−05	–	1.16E−04	–	1.61E−05	–	2.28E−05	–
	20	2.92E−06	3.60	1.29E−05	3.17	6.88E−08	7.87	9.73E−08	7.87
	40	1.91E−07	3.94	9.39E−07	3.78	2.75E−10	7.97	3.89E−10	7.97
	80	1.17E−08	4.02	5.10E−08	4.20	1.08E−12	7.99	1.53E−12	7.99
	160	6.60E−10	4.15	3.16E−09	4.01	4.30E−15	7.97	6.08E−15	7.97

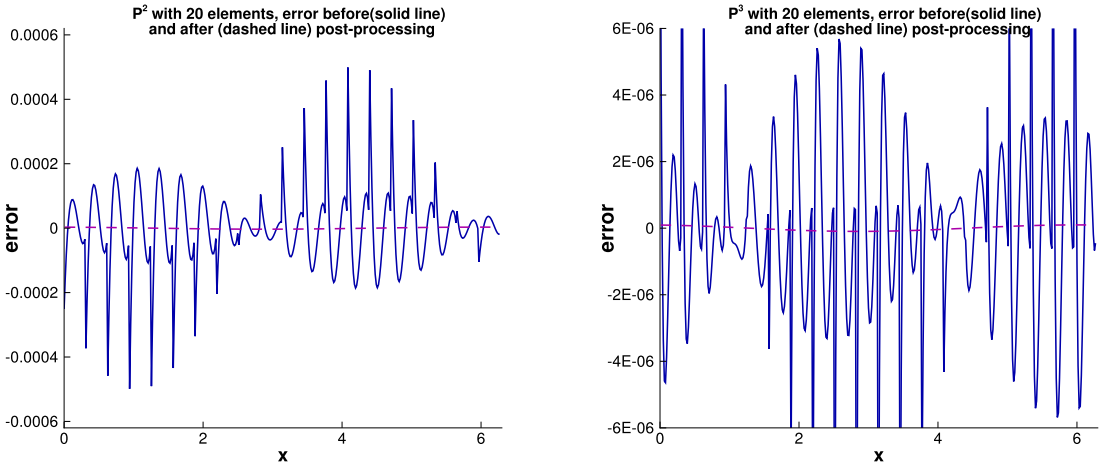

Fig. 5.1. Plots pointwise errors for linear Schrödinger equation in Example 5.1 before and after post-processing for 20 elements: P^2(left) and P^3(right).

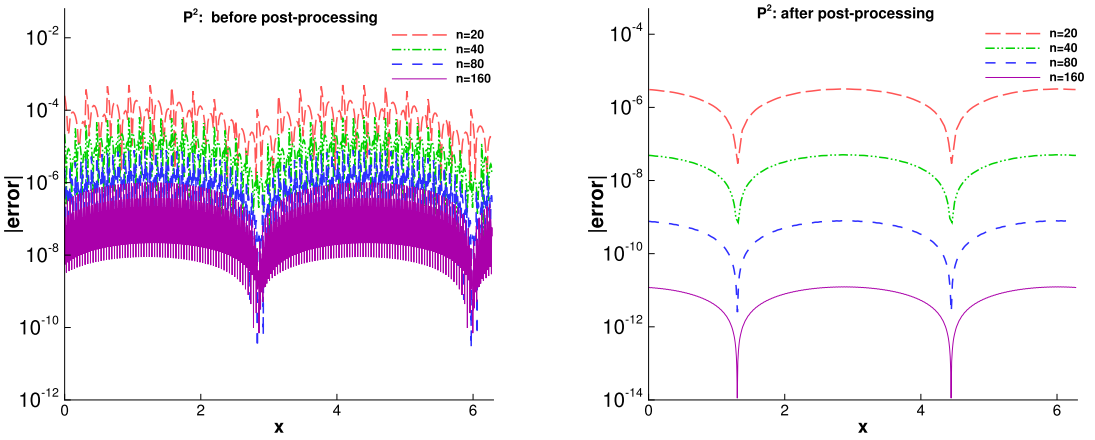

Fig. 5.2. The errors in absolute value and in logarithmic scale for linear Schrödinger equation in Example 5.1 for P^2 with N = 20, 40, 80, 160, before and after post-processing.

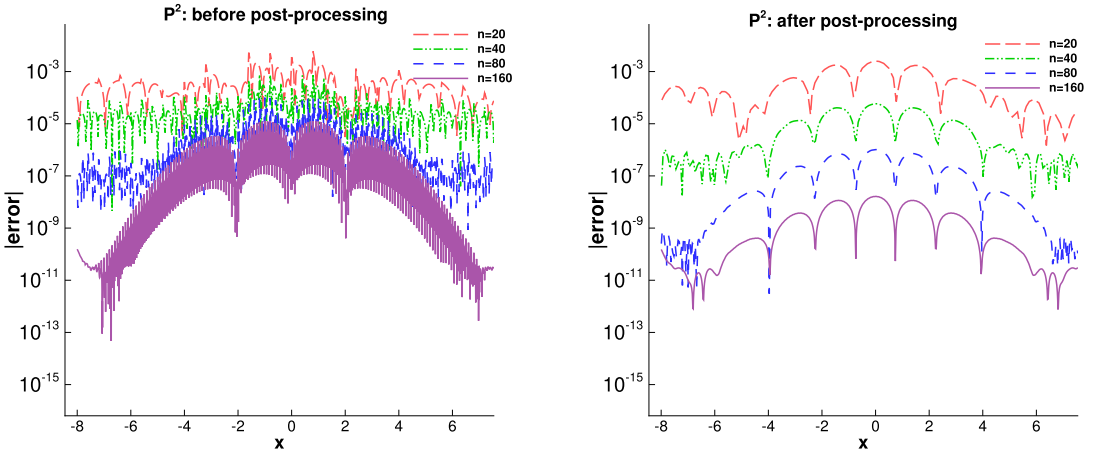

Fig. 5.3. The errors in absolute value and in logarithmic scale for variable coefficient Schrödinger equation in Example 5.2 for P^2 with n = 20, 40, 80, 160, before and after post-processing.

with the potential

$$V(x) = \frac{x^2}{2}.$$

With this potential it is easy to verify it supports the solution

$$u(x,t) = e^{-\frac{\sqrt{2}}{4}(x^2-2it)}, \quad (x,t) \in \Omega \times (0,T),$$

where $\Omega = [-8, 8]$ with periodic boundary conditions.

The errors and convergence rates are presented in Table 5.2, Fig. 5.3 and computed at time $T = 5$. Comparing the results with the linear case, the performance is very similar. In Table 5.2, we show the L^2 and L^∞ errors and convergence rates for this problem. Clearly, we can see the optimal convergence rate $k+1$ before post-processing and at least $2k+1$ after post-processing for P^k-elements in both L^2 and L^∞ norms. In Fig. 5.3, we plot the absolute errors in logarithmic scale before and after post-processing. It is found that the post-processed errors are less oscillatory and much smaller in magnitude.

Example 5.3. In this example, we consider nonlinear Schrödinger equation with a smooth solution in the domain $\Omega = [-35, 35]$:

$$iu_t + u_{xx} + 2|u|^2 u = 0, \quad \Omega \times (0,T),$$

Table 5.2
L^2- and L^∞-errors of real part and imaginary part of the equation shown in Example 5.2 before and after post-processing at time $T = 5$ using LDG method.

		Real part before post-processing				Real part after post-processing			
	N	L^2 error	Order	L^∞ error	Order	L^2 error	Order	L^∞ error	Order
P^1	20	9.53E−03	–	6.40E−03	–	8.38E−03	–	6.43E−03	–
	40	2.11E−03	2.17	1.67E−02	1.94	5.21E−04	4.01	5.00E−04	3.69
	80	5.34E−04	1.99	4.32E−03	1.95	3.32E−05	3.97	3.26E−05	3.94
	160	1.34E−04	2.00	1.09E−03	1.99	2.09E−06	3.99	2.06E−06	3.98
	320	3.34E−05	2.00	2.72E−04	2.00	1.31E−07	4.00	1.29E−07	4.00
P^2	20	7.91E−04	–	5.92E−03	–	3.20E−03	–	2.51E−03	–
	40	9.63E−05	3.04	8.07E−04	2.87	7.23E−05	5.47	5.85E−05	5.43
	80	1.02E−05	3.01	1.00E−04	3.01	1.25E−06	5.86	1.02E−06	5.84
	160	1.50E−06	2.99	1.26E−05	2.99	2.00E−08	5.96	1.64E−08	5.96
	320	1.88E−07	3.00	1.58E−06	3.00	3.26E−10	5.94	2.72E−10	5.91
P^3	10	4.44E−04	–	2.70E−03	–	6.48E−02	–	4.53E−02	–
	20	6.14E−05	2.86	4.99E−04	2.43	1.93E−03	5.07	1.48E−03	4.94
	40	4.35E−06	3.82	4.28E−05	3.54	1.56E−05	6.94	1.25E−05	6.88
	80	2.58E−07	4.08	2.58E−06	4.05	7.51E−08	7.70	6.08E−08	7.68
	160	1.72E−08	3.90	1.86E−07	3.80	3.21E−10	7.87	2.66E−10	7.83
		Imaginary part before post-processing				Imaginary part after post-processing			
	N	L^2 error	Order	L^∞ error	Order	L^2 error	Order	L^∞ error	Order
P^1	20	4.48E−03	–	2.70E−02	–	5.72E−03	–	3.83E−03	–
	40	1.02E−03	2.13	8.01E−03	1.75	3.29E−04	4.12	2.26E−04	4.08
	80	2.22E−04	2.20	1.81E−03	2.15	2.02E−05	4.03	1.39E−05	4.03
	160	5.55E−05	2.00	4.52E−04	2.00	1.27E−06	3.99	8.70E−07	3.99
	320	1.39E−05	2.00	1.13E−04	2.00	7.93E−08	4.00	5.44E−08	4.00
P^2	20	4.61E−04	–	2.58E−03	–	1.54E−03	–	1.01E−03	–
	40	5.42E−05	3.09	4.39E−04	2.56	2.99E−05	5.68	2.37E−05	5.41
	80	4.91E−06	3.46	4.16E−05	3.40	5.18E−07	5.85	4.14E−07	5.84
	160	6.24E−07	2.98	5.24E−06	2.99	8.30E−09	5.96	6.65E−09	5.96
	320	7.80E−08	3.00	6.56E−07	3.00	1.43E−10	5.86	9.59E−11	6.12
P^3	10	2.14E−04	–	9.16E−04	–	2.70E−02	–	1.89E−02	–
	20	3.17E−05	2.75	2.15E−04	2.09	8.01E−04	5.07	6.13E−04	4.94
	40	2.26E−06	3.81	1.64E−05	3.71	6.50E−06	6.94	5.20E−06	6.88
	80	1.08E−07	4.39	9.69E−07	4.08	3.12E−08	7.70	2.52E−08	7.69
	160	8.79E−09	3.62	7.97E−08	3.60	1.41E−10	7.79	9.44E−11	8.06

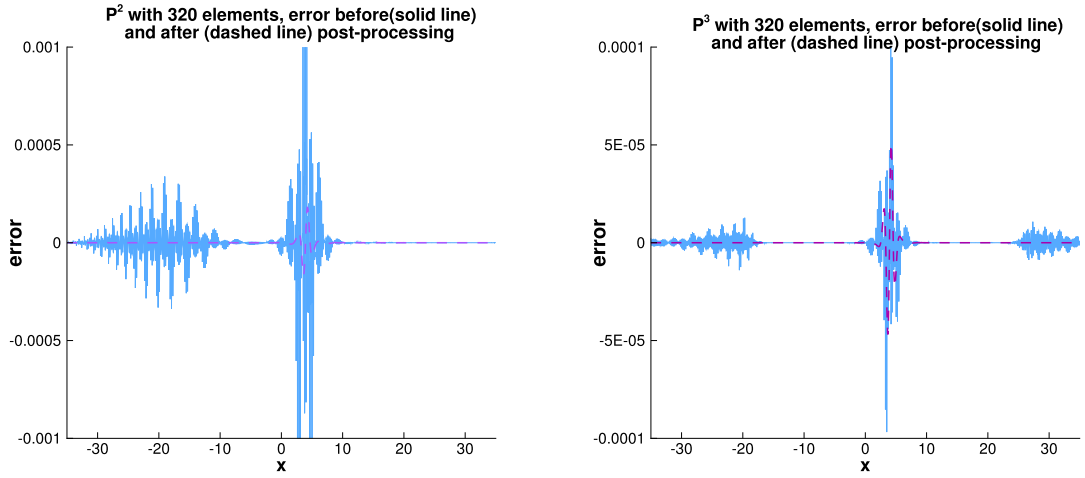

Fig. 5.4. Plots pointwise errors for nonlinear Schrödinger equation in Example 5.3 before and after post-processing for 320 elements: P^2(left) and P^3(right).

Table 5.3
L^2- and L^∞-errors of real part and imaginary part of nonlinear Schrödinger equation shown in Example 5.3 before and after post-processing at time $T = 1$ using LDG method.

		Real part before post-processing				Real part after post-processing			
	N	L^2 error	Order	L^∞ error	Order	L^2 error	Order	L^∞ error	Order
P^1	40	1.63E−01	–	1.08E+00	–	4.66E−01	–	9.58E−01	–
	80	7.92E−02	1.04	9.14E−01	0.24	2.10E−01	1.15	4.38E−01	1.13
	160	1.15E−02	2.78	1.47E−01	2.64	2.21E−02	3.25	4.93E−02	3.15
	320	1.94E−03	2.57	3.65E−02	2.01	1.22E−03	4.18	2.56E−03	4.27
	640	4.63E−04	2.07	9.05E−03	2.01	7.44E−05	4.03	1.58E−04	4.01
	1280	1.15E−04	2.00	2.25E−03	2.01	4.61E−06	4.01	9.86E−06	4.00
P^2	40	7.11E−02	–	5.73E−01	–	3.17E−01	–	6.69E−01	–
	80	9.26E−03	2.94	1.67E−01	1.78	5.54E−02	2.52	1.30E−01	2.37
	160	8.31E−04	3.48	1.54E−02	3.43	2.64E−03	4.39	6.84E−03	4.25
	320	9.75E−05	3.09	2.27E−03	2.76	6.28E−05	5.39	1.79E−04	5.26
	640	1.14E−05	3.10	3.00E−04	2.92	1.11E−06	5.82	3.27E−06	5.78
	1280	1.42E−06	3.00	3.79E−05	2.98	1.79E−08	5.95	5.30E−08	5.94
P^3	40	2.23E−02	–	2.84E−01	–	2.94E−01	–	5.85E−01	–
	80	1.48E−03	3.91	8.45E−03	5.07	5.30E−02	2.47	1.20E−01	2.29
	160	6.76E−05	4.46	1.28E−03	2.73	1.69E−03	4.97	4.63E−03	4.70
	320	4.19E−06	4.01	1.07E−04	3.58	1.64E−05	6.69	5.06E−05	6.51
	640	2.49E−07	4.07	6.77E−06	3.98	8.60E−08	7.57	2.78E−07	7.51
	1280	1.56E−08	4.00	4.21E−07	4.01	3.64E−10	7.88	1.19E−09	7.86
		Imaginary part before post-processing				Imaginary part after post-processing			
	N	L^2 error	Order	L^∞ error	Order	L^2 error	Order	L^∞ error	Order
P^1	40	1.63E−01	–	1.08E+00	–	4.00E−01	–	8.18E−01	–
	80	7.92E−02	1.04	9.14E−01	0.24	2.19E−01	0.87	3.86E−01	1.08
	160	1.15E−02	2.78	1.47E−01	2.64	2.29E−02	3.26	4.66E−02	3.05
	320	1.94E−03	2.57	3.65E−02	2.01	1.25E−03	4.19	2.42E−03	4.27
	640	4.63E−04	2.07	9.05E−03	2.01	7.62E−05	4.03	1.53E−04	3.98
	1280	1.15E−04	2.00	2.25E−03	2.01	4.72E−06	4.01	9.48E−06	4.01
P^2	40	7.11E−02	–	5.73E−01	–	2.90E−01	–	5.94E−01	–
	80	9.26E−03	2.94	1.67E−01	1.78	5.59E−02	2.58	1.29E−01	2.21
	160	8.31E−04	3.48	1.54E−02	3.43	2.64E−03	4.50	7.57E−03	4.09
	320	9.75E−05	3.09	2.27E−03	2.76	6.30E−05	5.39	1.97E−04	5.26
	640	1.14E−05	3.10	3.00E−04	2.92	1.11E−06	5.82	3.59E−06	5.78
	1280	1.42E−06	3.00	3.79E−05	2.98	1.80E−08	5.95	5.84E−08	5.94
P^3	40	2.23E−02	–	2.84E−01	–	2.93E−01	–	5.93E−01	–
	80	1.48E−03	3.91	8.45E−03	5.07	5.27E−02	2.48	1.21E−01	2.29
	160	6.76E−05	4.46	1.28E−03	2.73	1.70E−03	4.96	4.96E−03	4.61
	320	4.19E−06	4.01	1.07E−04	3.58	1.64E−05	6.69	5.45E−05	6.51
	640	2.49E−07	4.07	6.77E−06	3.98	8.62E−08	7.57	3.01E−07	7.50
	1280	1.56E−08	4.00	4.21E−07	4.01	3.65E−10	7.88	1.29E−09	7.86

with the soliton solution

$$u(x,t) = sech(x-4t)exp(2i(cx-\frac{3}{2}t)),$$

with periodic boundary conditions.

The errors and convergence rates are presented in Table 5.3 and Figs. 5.4, 5.5 and computed at time $T = 1$. Although not proven in this paper, we expect the same accuracy results to hold for LDG solutions as in Examples 5.1 and 5.2. In Table 5.3 it shows that for the nonlinear case we obtain the optimal $k+1$ order of accuracy before post-processing and at least $2k+1$ order of accuracy after post-processing for P^k-elements in both the L^2- and L^∞-norms. In Fig. 5.4 we plot the errors of the numerical errors before and after processing for P^2 and P^3 cases with 320 elements. Similarly, we see that the error before post-processing is highly oscillatory, and the post-processing gets rid of the oscillatory in the error and greatly reduces its magnitude. In Fig. 5.5 we plot the errors, in absolute value in logarithmic scale of the numerical solution before and after post-processing in $[-10, 10]$, with $n = 160, 320, 640, 1280$. We find that the post-processed errors are less oscillatory and much smaller in magnitude. However, notice that due to nonlinear effects not all oscillations in the errors have been removed by post-processing, especially for a large number of elements.

Example 5.4. In this example, we consider two dimensional Schrödinger equation with a smooth solution in the domain $\Omega = [-8, 8] \times [-8, 8]$

$$iu_t = -\frac{1}{2}(u_{xx} + u_{yy}) + V(x,y)u, \quad \Omega \times (0,T),$$

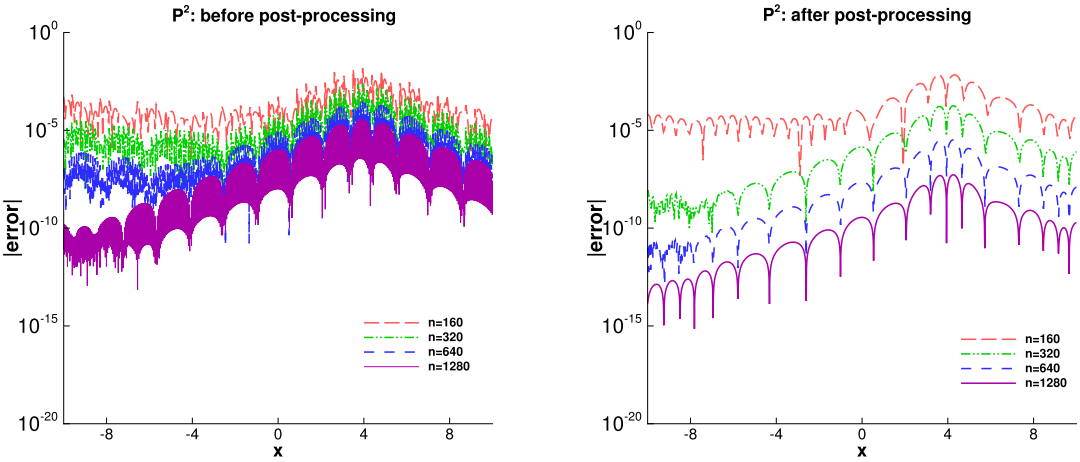

Fig. 5.5. The errors in absolute value and in logarithmic scale for nonlinear Schrödinger equation in Example 5.3 in $[-10,10]$, for P^2 with $n = 20, 40, 80, 160$, before and after post-processing.

Table 5.4
L^2- and L^∞-errors of real part and imaginary part of the 2D Schrödinger equation shown in Example 5.4 before and after post-processing at time $T = 1$ using LDG method. We can see at least $\mathscr{O}(h^{2k+1})$ in both the L^2- and L^∞-norms.

		Real part before post-processing				Real part after post-processing			
	N	L^2 error	Order	L^∞ error	Order	L^2 error	Order	L^∞ error	Order
P^1	20 × 20	4.22E−03	–	1.17E−01	–	2.19E−02	–	1.17E−02	–
	40 × 40	9.52E−04	2.15	2.78E−02	2.08	2.07E−03	3.40	1.13E−03	3.38
	80 × 80	2.06E−04	2.21	7.45E−03	1.90	7.20E−05	4.85	7.00E−05	4.01
	160 × 160	4.77E−05	2.11	1.80E−03	2.05	4.20E−06	4.10	4.45E−06	3.97
	320 × 320	1.19E−05	2.00	4.50E−04	2.00	2.63E−07	4.00	2.80E−07	3.99
P^2	10 × 10	4.10E−03	–	9.86E−02	–	1.24E−01	–	9.57E−02	–
	20 × 20	4.09E−04	3.32	7.85E−03	3.65	7.94E−03	3.96	6.81E−03	3.81
	40 × 40	4.49E−05	3.19	1.35E−03	2.54	1.99E−04	5.32	1.83E−04	5.22
	80 × 80	7.30E−06	2.62	1.67E−04	3.02	3.57E−06	5.80	3.32E−06	5.78
	160 × 160	9.02E−07	3.02	2.00E−05	3.06	5.78E−08	5.95	5.41E−08	5.94
P^3	10 × 10	1.89E−04	–	2.85E−03	–	1.22E−01	–	9.03E−02	–
	20 × 20	3.77E−05	2.32	1.22E−03	1.23	5.52E−03	4.46	4.76E−03	4.25
	40 × 40	2.04E−06	4.21	7.50E−05	4.02	5.69E−05	6.60	5.21E−05	6.51
	80 × 80	1.25E−07	4.04	5.28E−06	3.83	2.96E−07	7.59	2.76E−07	7.56
	160 × 160	8.98E−09	3.79	3.98E−07	3.73	1.24E−09	7.89	1.17E−09	7.89
		Imaginary part before post-processing				Imaginary part after post-processing			
	N	L^2 error	Order	L^∞ error	Order	L^2 error	Order	L^∞ error	Order
P^1	20 × 20	4.77E−03	–	1.47E−01	–	2.76E−02	–	1.99E−02	–
	40 × 40	1.41E−03	1.76	4.81E−02	1.61	2.32E−03	3.57	1.54E−03	3.69
	80 × 80	2.96E−04	2.25	1.13E−02	2.09	1.07E−04	4.44	1.03E−04	3.90
	160 × 160	7.43E−05	1.99	2.80E−03	2.01	6.73E−06	3.99	6.61E−06	3.97
	320 × 320	1.86E−05	2.00	7.01E−04	2.00	4.22E−07	4.00	4.15E−07	3.99
P^2	10 × 10	6.47E−03	–	1.71E−01	–	1.90E−01	–	1.43E−01	–
	20 × 20	5.45E−04	3.57	1.19E−02	3.85	1.21E−02	3.97	1.05E−02	3.76
	40 × 40	7.70E−05	2.82	2.11E−03	2.49	3.13E−04	5.27	2.83E−04	5.22
	80 × 80	8.55E−06	3.17	2.59E−04	3.03	5.54E−06	5.82	5.15E−06	5.78
	160 × 160	1.07E−06	3.00	3.15E−05	3.04	8.96E−08	5.95	8.37E−08	5.94
P^3	10 × 10	2.12E−04	–	3.43E−03	–	1.89E−01	–	1.41E−01	–
	20 × 20	4.72E−05	2.17	1.67E−03	1.04	8.59E−03	4.46	7.40E−03	4.25
	40 × 40	3.38E−06	3.81	1.47E−04	3.50	8.86E−05	6.60	8.12E−05	6.51
	80 × 80	2.13E−07	3.98	1.03E−05	3.83	4.60E−07	7.59	4.30E−07	7.56
	160 × 160	1.35E−08	3.99	6.71E−07	3.95	1.94E−09	7.89	1.82E−09	7.88

with the potential

$$V(x) = \frac{x^2 + y^2}{2}.$$

We take the exact solution to be

$$u(x, t) = e^{-it} e^{-\frac{x^2+y^2}{2}}.$$

In this example we use the $\mathcal{Q}^k$ polynomial approximation space in the LDG method. The L^2 and L^∞ errors and convergence rates are presented in Table 5.4 at time $T = 1$. Similarly, we see that after post-processing the order of accuracy has been improved from $\mathcal{O}(h^{k+1})$ to at least $\mathcal{O}(h^{2k+1})$.

6. Conclusions

In this paper we have proved the optimal L^2-error estimate of the local discontinuous Galerkin (LDG) method for variable coefficient Schrödinger equations. We have also established the existence of higher order of accuracy of the LDG method to variable coefficient Schrödinger equations in the negative-order norm. The divided difference estimates are straight forward from the estimates of the LDG solution itself. Based on these theoretical results, by using the SIAC filter we can improve the accuracy of LDG approximation from $\mathcal{O}(h^{k+1})$ to at least $\mathcal{O}(h^{2k})$, when the alternating numerical fluxes are adopted in the method. The convergence rate of LDG solutions was demonstrated by the numerical tests. Furthermore these results and technique can be easily extend to high dimensional space following the same ideas. But for the nonlinear case, although we can get the same numerical results as in the linear and variable coefficient cases, it is nontrivial in the theoretical demonstration. So we leave this for the future work.

References

[1] Y. Xu, C.-W. Shu, Local discontinuous Galerkin methods for nonlinear Schrödinger equations, J. Comput. Phys. 205 (1) (2005) 72–97.
[2] Y. Xu, C.-W. Shu, Optimal error estimates of the semidiscrete local discontinuous Galerkin methods for high order wave equations, SIAM J. Numer. Anal. 50 (1) (2012) 79–104.
[3] W. Reed, T. Hill, Triangular Mesh Methods for the Neutron Transport Equation, La-ur-73-479, Los Alamos Scientific Laboratory, 1973.
[4] B. Cockburn, C.-W. Shu, The local discontinuous Galerkin method for time-dependent convection-diffusion systems, SIAM J. Numer. Anal. 35 (6) (1998) 2440–2463.
[5] B. Cockburn, G.E. Karniadakis, C.-W. Shu, The development of discontinuous Galerkin methods, in: B. Cockburn, G. Karniadakis, C.-W. Shu (Eds.), Discontinuous Galerkin Methods: Theory, Computation and Applications, in: Lecture Notes in Computational Science and Engineering, vol. 11, Springer, 2000, pp. 3–50, Part I: Overview.
[6] B. Riviere, Discontinuous Galerkin Methods for Solving Elliptic and Parabolic Equations: Theory and Implementation, Society for Industrial and Applied Mathematics, 2008.
[7] Y. Xu, C.-W. Shu, Local discontinuous Galerkin methods for high-order time-dependent partial differential equations, Commun. Comput. Phys. 7 (1) (2010) 1–46.
[8] C.-W. Shu, Discontinuous Galerkin method for time dependent problems: Survey and recent developments, in: X. Feng, O. Karakashian, Y. Xing (Eds.), Recent Developments in Discontinuous Galerkin Finite Element Methods for Partial Differential Equations (2012 John H. Barrett Memorial Lectures), in: The IMA Volumes in Mathematics and Its Applications, vol. 157, Springer, Switzerland, 2014, pp. 25–62.
[9] J.H. Bramble, A.H. Schatz, Higher order local accuracy by averaging in the finite element method, Math. Comp. 31 (137) (1997) 94–111.
[10] V. Thomée, High order local approximations to derivatives in the finite element method, Math. Comp. 31 (139) (1997) 652–660.
[11] M.S. Mock, P.D. Lax, The computation of discontinuous solutions of linear hyperbolic equations, Comm. Pure Appl. Math. 31 (4) (1978) 423–430.
[12] B. Cockburn, M. Luskin, C.-W. Shu, E. Süli, Enhanced accuracy by post-processing for finite element methods for hyperbolic equations, Math. Comp. 72 (242) (2003) 577–606.
[13] J.K. Ryan, C.-W. Shu, On a one-sided post-processing technique for the discontinuous Galerkin methods, Methods Appl. Anal. 10 (2) (2003) 295–308.
[14] M. Steffen, S. Kirby, R.M. Kirby, J.K. Ryan, Investigation of smoothness-increasing accuracy-conserving filters for improving streamline integration through discontinuous fields, IEEE Trans. Vis. Comput. Graphics 14 (3) (2008) 680–692.
[15] P. van Slingerland, J.K. Ryan, C. Vuik, Position-dependent smoothness-increasing accuracy-conserving (SIAC) filtering for improving discontinuous Galerkin solutions, SIAM J. Sci. Comput. 33 (2) (2011) 802–825.
[16] S. Curtis, R.M. Kirby, J.K. Ryan, C.-W. Shu, Postprocessing for the discontinuous Galerkin method over nonuniform meshes, SIAM J. Sci. Comput. 30 (1) (2007) 272–289.
[17] H. Mirzaee, L. Ji, J.K. Ryan, R.M. Kirby, Smoothness-increasing accuracy-conserving (SIAC) postprocessing for discontinuous Galerkin solutions over structured triangular meshes, SIAM J. Numer. Anal. 49 (5) (2011) 1899–1920.
[18] H. Mirzaee, J. King, J.K. Ryan, R.M. Kirby, Smoothness-increasing accuracy-conserving filters for discontinuous Galerkin solutions over unstructured triangular meshes, SIAM J. Numer. Anal. 35 (1) (2013) A212–A230.
[19] H. Mirzaee, J.K. Ryan, R.M. Kirby, Smoothness-increasing accuracy-conserving (SIAC) filters for discontinuous Galerkin solutions: Application to structured tetrahedral meshes, J. Sci. Comput. 58 (3) (2014) 690–704.
[20] L. Ji, Y. Xu, J.K. Ryan, Negative-order norm estimates for nonlinear hyperbolic conservation laws, J. Sci. Comput. 54 (2–3) (2013) 531–548.
[21] X. Meng, J.K. Ryan, Discontinuous Galerkin methods for nonlinear scalar hyperbolic conservation laws: divided difference estimates and accuracy enhancement, Numer. Math. 136 (1) (2017) 27–73.
[22] J.K. Ryan, C.-W. Shu, H. Atkins, Extension of a post processing technique for the discontinuous Galerkin method for hyperbolic equations with application to an aeroacoustic problem, SIAM J. Sci. Comput. 26 (3) (2005) 821–843.
[23] J.K. Ryan, B. Cockburn, Local derivative post-processing for the discontinuous Galerkin method, J. Comput. Phys. 228 (23) (2009) 8642–8664.
[24] X. Li, J.K. Ryan, R.M. Kirby, C. Vuik, Smoothness-increasing accuracy-conserving (SIAC) filters for derivative approximations of discontinuous Galerkin (DG) solutions over nonuniform meshes and near boundaries, J. Comput. Appl. Math. 294 (2016) 275–296.
[25] L. Ji, Y. Xu, J.K. Ryan, Accuracy-enhancement of discontinuous Galerkin solutions for convection-diffusion equations in multiple-dimensions, Math. Comp. 81 (280) (2012) 1929–1950.

[26] D. Walfisch, J.K. Ryan, R.M. Kirby, R. Haimes, One-sided smoothness-increasing accuracy-conserving filtering for enhanced streamline integration through discontinuous fields, J. Sci. Comput. 38 (2) (2009) 164–184.
[27] L. Zhou, Y. Xu, Z. Zhang, W. Cao, Superconvergence of local discontinuous Galerkin method for one-dimensional linear Schrödinger equations, J. Sci. Comput. 73 (2017) 1290–1315.
[28] J. Wang, Y. Huang, Z. Tian, J. Zhou, Superconvergence analysis of finite element method for the time-dependent Schrödinger equation, Math. Appl. 71 (10) (2016) 1960–1972.
[29] D. Shi, X. Liao, L. Wang, A nonconforming quadrilateral finite element approximation to nonlinear Schrödinger equation, Acta Math. Sci. 37 (3) (2017) 584–592.
[30] J. Yan, C.-W. Shu, A local discontinuous Galerkin method for KdV type equations, SIAM J. Numer. Anal. 40 (2) (2002) 769–791.
[31] P.G. Ciarlet, The Finite Element Method for Elliptic Problems, Society for Industrial and Applied Mathematics, 2002.
[32] X. Meng, C.-W. Shu, B, Wu optimal error estimates for discontinuous Galerkin methods based on upwind-biased fluxes for linear hyperbolic equations, Math. Comp. 85 (299) (2016) 1225–1261.
[33] B. Cockburn, G. Kanschat, I. Perugia, D. Schötzau, Superconvergence of the local discontinuous Galerkin method for elliptic problems on Cartesian grids, SIAM J. Numer. Anal. 39 (1) (2001) 264–285.